CR-171 781

(N84-10150) UNDERSTANDING AND UTILIZATION OF THEMATIC MAPPER AND OTHER REMOTELY SENSED DATA FOR VEGETATION MONITORING Final Report, 1 Nov. 1982 - 31 Oct. 1983 (Environmental Research Inst. of Michigan) G3/43

N84-26098

Unclas 00150

160300-76-F

Final Report

UNDERSTANDING AND UTILIZATION OF THEMATIC MAPPER AND OTHER REMOTELY SENSED DATA FOR VEGETATION MONITORING

E.P. CRIST, R.C. CICONE, M.D. METZLER, T.M. PARRIS, D.P. RICE AND R.E. SAMPSON

Infrared and Optics Division

NOVEMBER 1983

Earth Sciences and Applications Division
NASA/Johnson Space Center
Houston, Texas 77058
Contract No. NAS9-16538

ENVIRONMENTAL
RESEARCH INSTITUTE OF MICHIGAN
BOX 8618 • ANN ARBOR • MICHIGAN 48107

TECHNICAL REPORT STANDARD TITLE PAGE

1. Report No.	2. Government Accession No.	3. Recipient's Catalog No.
160300-76-F		

4. Title and Subtitle	5. Report Date
Understanding and Utilization of Thematic Mapper and Other Remotely Sensed Data for Vegetation Monitoring	November 1983
	6. Performing Organization Code
7. Author(s) E.P. Crist, R.C. Cicone, M.D. Metzler T.M. Parris, D.P. Rice and R.E. Sampson	8. Performing Organization Report No. 160300-76-F
9. Performing Organization Name and Address Environmental Research Institute of Michigan P.O. Box 8618 Ann Arbor, MI 48107	10. Work Unit No.
	11. Contract or Grant No. NAS9-16538
	13. Type of Report and Period Covered Final Report 1 November 1982 through 31 October 1983
12. Sponsoring Agency Name and Address Earth Sciences and Applications Division NASA/Johnson Space Center Houston, Texas 77058	14. Sponsoring Agency Code

15. Supplementary Notes
Mr. Lewis C. Wade and Dr. Victor S. Whitehead served as NASA Technical Monitors of the reported effort.

16. Abstract

This document is a final progress report for FY83 ERIM research activities in support of the Earth Sciences and Applications Division, NASA Johnson Space Center, primarily concerned with understanding and using Thematic Mapper data. The TM Tasseled Cap transformation, which provides both a 50% reduction in data volume with little or no loss of important information and spectral features with direct physical association, is presented and discussed. Using both simulated and actual TM data, some important characteristics of vegetation and soils in this feature space are described, as are the effects of solar elevation angle and atmospheric haze. A preliminary spectral haze diagnostic feature, based on only simulated data, is also described. The characteristics of the TM thermal band are discussed, as is a demonstration of the use of TM data in energy balance studies. Finally, some characteristics of AVHRR data are described, as are the sensitivities to scene content of several Landsat-MSS preprocessing techniques.

17. Key Words	18. Distribution Statement
Landsat, Thematic Mapper, Tasseled Cap Transformation, Spectral Features, Atmospheric Effects, Atmospheric Correction, Soil Reflectance, Soil Properties, Thermal Band, Energy Balance, Preprocessing, AVHRR, Remote Sensing, Vegetation Monitoring, Agricultural Remote Sensing	

19. Security Classif. (of this report)	20. Security Classif. (of this page)	21. No. of Pages	22. Price
Unclassified	Unclassified	xii + 92	

160300-76-F

Final Report

UNDERSTANDING AND UTILIZATION OF THEMATIC MAPPER AND OTHER REMOTELY SENSED DATA FOR VEGETATION MONITORING

by

E.P. Crist, R.C. Cicone, M.D. Metzler,
T.M. Parris, D.P. Rice and R.E. Sampson

This report describes results of research performed in support of the Earth Sciences and Applications Division, NASA Johnson Space Center. Section 6.0 describes activities carried out wholly or in part under the auspices of the AgRISTARS program.

Environmental Research Institute of Michigan
P.O. Box 8618
Ann Arbor, Michigan 48107

November 1983

TABLE OF CONTENTS

TABLE OF CONTENTS (Continued)

LIST OF FIGURES

LIST OF FIGURES (Continued)

LIST OF TABLES

PREFACE

This report describes part of a comprehensive and continuing program of research concerned with advancing the state-of-the-art in remote sensing of the environment from aircraft and satellites. The research is being carried out for the Earth Sciences and Applications Division of NASA's Lyndon B. Johnson Space Center, Houston, Texas, by the Environmental Research Institute of Michigan (ERIM). Dr. Jon D. Erickson is the Division Chief and Mr. James L. Dragg is Chief of the Remote Sensing Research Branch. Mr. Lewis C. Wade, and subsequently, Dr. Victor S. Whitehead served as Technical Coordinators of the reported effort. The basic objective of this multidisciplinary program is to develop remote sensing as a practical tool to provide the scientist, planner and decision-maker with extensive information quickly and economically.

Timely information obtained by remote sensing can be directly important to such people as the farmer, the city planner, the conservationist and others concerned with problems such as crop yield and disease, urban land studies and development, water pollution and forest management. In a longer range view, remote sensing is one of a number of tools applicable to developing an understanding of the more global physical processes affecting the earth. The scope of our program includes:

1. Extending the understanding of basic processes.
2. Discovering new applications, developing advanced remote-sensing systems, and improving automatic data processing to extract information in a useful form.
3. Assisting in data collection, processing, analysis, and ground-truth verification.

The research described herein was performed under NASA Contract NAS9-16538 by ERIM's Infrared and Optics Division headed by Jack L. Walker, Vice-President of ERIM, under the direction of Robert Horvath, Program Manager and Eric Crist, Technical Director.

1.0
INTRODUCTION

This final report describes progress made by the Environmental Research Institute of Michigan (ERIM) in support of the Earth Sciences and Applications Division, NASA Johnson Space Center, during the period 1 November 1982 through 31 October 1983. Research conducted in this time period covered a range of topics in support of NASA/JSC's AgRISTARS and LIDQA efforts, as well as other of their ongoing research activities.

The task structure under which the reported work was carried out was modified part-way through the contract year to accomodate changes in the primary directions and emphases of research in the Earth Sciences and Applications Division. The modified tasks, as described in Section 1.1, will provide the basic structure for this report, while work carried out in earlier tasks will be grouped together in another section of the report.

1.1 TASKS AND OBJECTIVES

ERIM's research effort is organized into four tasks:

1. Thematic Mapper Feature Space Analysis
2. Thematic Mapper External Effects Analysis
3. Thematic Mapper Target Signature Characterization
4. Thematic Mapper Thermal Band Investigations

These four tasks are intended to provide increased understanding of the characteristics of TM data in the reflective and thermal bands, and to achieve initial understanding of the expression in those data of vegetation and soil characteristics, as well as the influence of external effects on the data.

Task 1 aims at understanding the dimensionality of data from the six reflective TM bands (Bands 1 through 5 and 7) and the distribution of those data in the six-dimensional space defined by the sensor bands.

Using this understanding, the task is intended to develop a preliminary transformation of actual TM data which will: a) align the data such that the dimensional relationships present might be most readily accessible to view and b) orient the data to provide features which have direct association to physical properties of scene classes.

Task 2 seeks to understand the effect of haze and sun elevation angle on TM data, particulary on TM Tasseled Cap features, and to devise preliminary methods by which those effects can be corrected or normalized.

The goal of Task 3 is to understand patterns of vegetative development as expressed in TM Tasseled Cap feature space, and to determine the expression of some key vegetation and soil conditions in that space.

Finally, Task 4 seeks to develop understanding of the characteristics of the TM thermal band, to investigate the areas in which TM thermal data might be of greatest use, and to demonstrate methods of applying TM data to both local and global energy balance problems.

Additional research reported here concerns the effects of preprocessing on MSS data, with the goal of understanding how various schemes affect data integrity and interpretability. In addition, analysis of the characteristics of data from the AVHRR (Advanced Very High Resolution Radiometer) on the NOAA satellites, and the potential for joint use of AVHRR and MSS data, are discussed.

1.2 SUMMARY OF PROGRESS

Substantial progress has been made toward achieving the objectives of the identified tasks. It should be noted, however, that all four tasks in the current structure are intended to extend into FY84, and are as a result not yet completed.

Work in Task 1, TM Feature Space Analysis, has resulted in a preliminary TM Tasseled Cap transformation for actual TM data, as well

as considerable progress in our understanding of the characteristics of the features of this transformation and the physical scene characteristics to which they respond. Section 2 provides a more detailed discussion of these results.

In Task 2, TM External Effects Analysis, FY83 progress includes initial characterization of haze and sun elevation angle effects on TM Tasseled Cap features based on simulation using data from the Dave atmospheric model. A comparison of the Dave and Turner models has been largely completed, with the goal of understanding their relative performance so that the more flexible Turner model may be used to supplement results obtained with the Dave model data sets. Finally, a preliminary haze diagnostic feature has been developed based on the simulated data analysis. Section 3 describes the technical effort in greater detail.

Progress in Task 3, TM Target Signature Characterization, has included derivation of a simple feature relating TM Tasseled Cap data to the percent of vegetation in a scene element, and description of the patterns of vegetative development both in general terms and for particular cover types. Section 4 describes this work.

Task 4, TM Thermal Band Investigations, has achieved a general description, through modeling, of the effects and interactions of atmospheric conditions, view angle, and target temperature on TM thermal band data. In addition, analysis techniques for calculating local and global energy balance have been devised and demonstrated on an actual TM scene. These results are discussed in Section 5.

The effects of Various preprocessing schemes on the ability to distinguish various cover types and to interpret spectral features were determined as a follow-on study to one carried out in FY82 [1]. Finally, basic understanding of the characteristics of the AVHRR was developed, including development of a simple geometric model to account for scan angle effects. These studies are described in Section 6. Table 1.1 summarizes the major accomplishments of ERIM's FY83 research.

TABLE 1.1. MAJOR ACCOMPLISHMENTS OF ERIM FY83 RESEARCH

- Tasseled Cap transformation for actual TM Data developed
- Haze, sun angle effects quantified for simulated data
- Preliminary haze diagnostic feature developed
- General and specific vegetation development profiles derived in TM Tasseled Cap feature space
- External effects on the TM thermal band described
- Analysis techniques for calculating local and global energy balance developed
- AVHRR data characteristics described, geometric correction model developed

2.0
THEMATIC MAPPER FEATURE SPACE ANALYSIS

The successful launch of Landsat-4, which carries the Thematic Mapper (TM) as well as the Multispectral Scanner (MSS), signaled the start of new phase in the land remote sensing program. The TM records data in a larger number of spectral bands which cover a broader portion of the electromagnetic spectrum, as well as providing finer quantization, improved signal-to-noise ratio, and higher spatial resolution. This task is intended to achieve understanding of the spectral characteristics of TM data - in particular with regard to their dimensionality - and to derive features which facilitate extraction of the crop and soils related information contained in those data.

2.1 BACKGROUND

Work toward understanding the dimensionality and features of TM data was begun in FY82 using simulated TM data [1]. These analyses revealed that data from the six reflective TM bands primarily occupy three dimensions (containing 99% of the total variability in the simulated data set), and further define two planes (or more accurately plane-like data concentrations) in that three dimensional space. Figure 2.1 illustrates this data dispersion. A transformation, named the TM Tasseled Cap, was derived which applied a multidimensional linear rotation to the simulated data such that the plane-like data concentrations were most readily accessible to view. This transformation also defined the feature space such that spectral response could be directly associated with physical characteristics of scene classes.

In the TM Tasseled Cap transformation, the Plane of Vegetation (Figure 2.1) is defined by Brightness and Greenness, which are comparable and virtually identical, respectively, to the MSS Tasseled

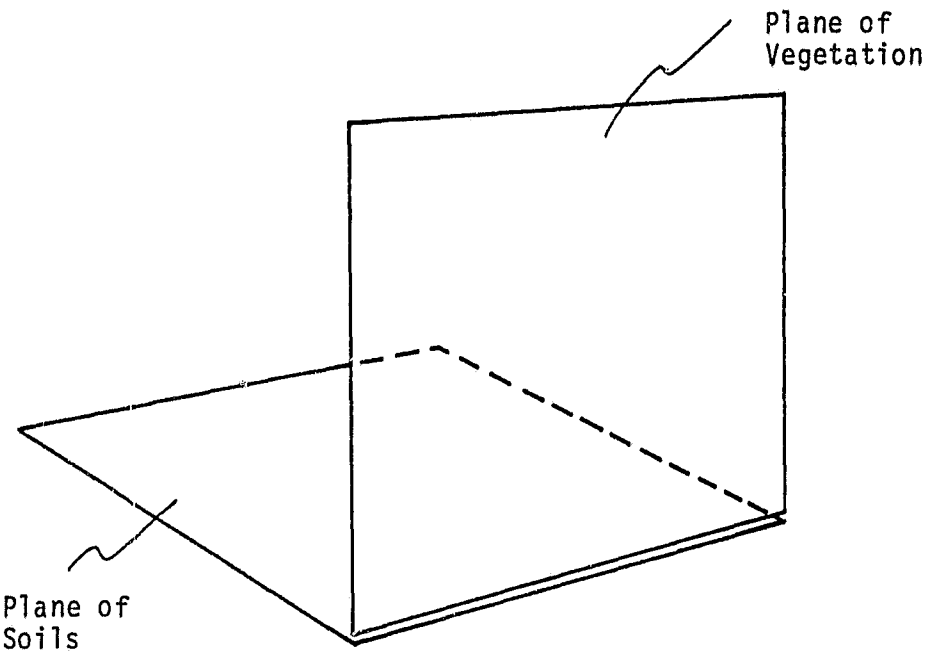

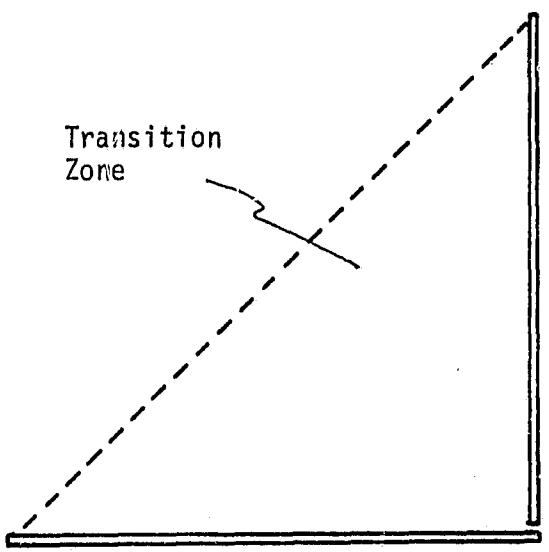

FIGURE 2.1. BASIC SPECTRAL STRUCTURE OF TM DATA

Cap features. Thus practically speaking, the TM Plane of Vegetation is equivalent to the MSS data plane. The Plane of Soils and Transition Zone views of Figure 2.1 include a third feature, which represents the majority of new information in the TM data, largely associated with the longer infrared TM bands. This third feature showed indications, in the simulated data, of being responsive to soil moisture variation in data taken from bare soils. The simulated data analyses are described in greater detail in references [1-3].

2.2 REAL DATA TRANSFORMATION

Although the simulation of TM data used in the previously described analyses was demonstrated to be reasonably accurate [2], some variations between simulated and actual data should be expected. As a result, derivation of a TM Tasseled Cap transformation for actual data would likely require some adjustment of the simulation-based transformation. The process by which that adjustment was accomplished is described in this section.

2.2.1 DATA

The data set used in this analysis consisted of portions of three TM scenes, as described in Table 2.1. All three sub-scenes contain some proportion of agricultural fields, natural vegetation, forest, water and manmade features (e.g., roads, airports, urban areas). The North Carolina scene, which includes an extensive agricultural holding with unusually large fields surrounded by forest and water, constitutes an ideal scene for derivation of a data transformation, since it provides a diverse set of cover types in a small area. As a result, this scene served as the primary study site, while the other two sites were used to confirm the results obtained for the North Carolina scene. Samples ranging from 1-in-25 to 1-in-225 were selected, resulting in

TABLE 2.1. DESCRIPTION OF THEMATIC MAPPER DATA SETS

Scene Name	Scene #	Date	Sub-scene Lines	Sub-scene Points
Arkansas/Tennessee	40037-16031	22 Aug '82	1-1600	2975-4775
Iowa	40049-16262	03 Sep '82	1-965	1990-4235
North Carolina	40070-15084	24 Sep '82	1755-2225	3125-3810

9000-13000 pixel samples from the three scenes. These samples constituted the actual data sets used in the analysis.

2.2.2 RESULTS

Direct application of the simulation-based coefficients to the actual TM data produced data presentations in which the basic dimensional relationships were detectable, but with slight skews with respect to the intended feature axes. A series of small rotations (less than 10^0 each) was applied to adjust the data such that the correct alignment with feature axes was obtained. Figure 2.2 illustrates the resulting data distributions for the North Carolina agricultural scene. The associated transformation coefficients, provided in Table 2.2, produced comparable results for the other two actual TM scenes. It will be noted that in Table 2.2, the third feature of the transformation is denoted as "Wetness". The reason for this name assignment will be discussed in Section 2.3.

As with the simulated data, the first three TM Tasseled Cap features contain the vast majority of total data variability (99% in the data pictured in Figure 2.2). Comparison of TM and MSS Tasseled Cap features for the same North Carolina site (carried out for NASA/GSFC) have shown that, as with the simulated data, TM and MSS Greenness are virtually identical (correlation of greater than .99), while the Brightness features are very similar but <u>not</u> identical (correlation of .75) [4]. As a result of these and other findings discussed in Section 2.3, we believe that the conclusions reached with regard to the simulated TM data analyses [1-3] can be applied to actual TM data as well.

While the limited data set used necessitates the labeling of the real data TM Tasseled Cap transformation as preliminary, the transformation nonetheless provides a means by which: a) substantial data volume reduction can be achieved with minimal loss of information, b) the data concentrations resulting from intrinsic reflectance

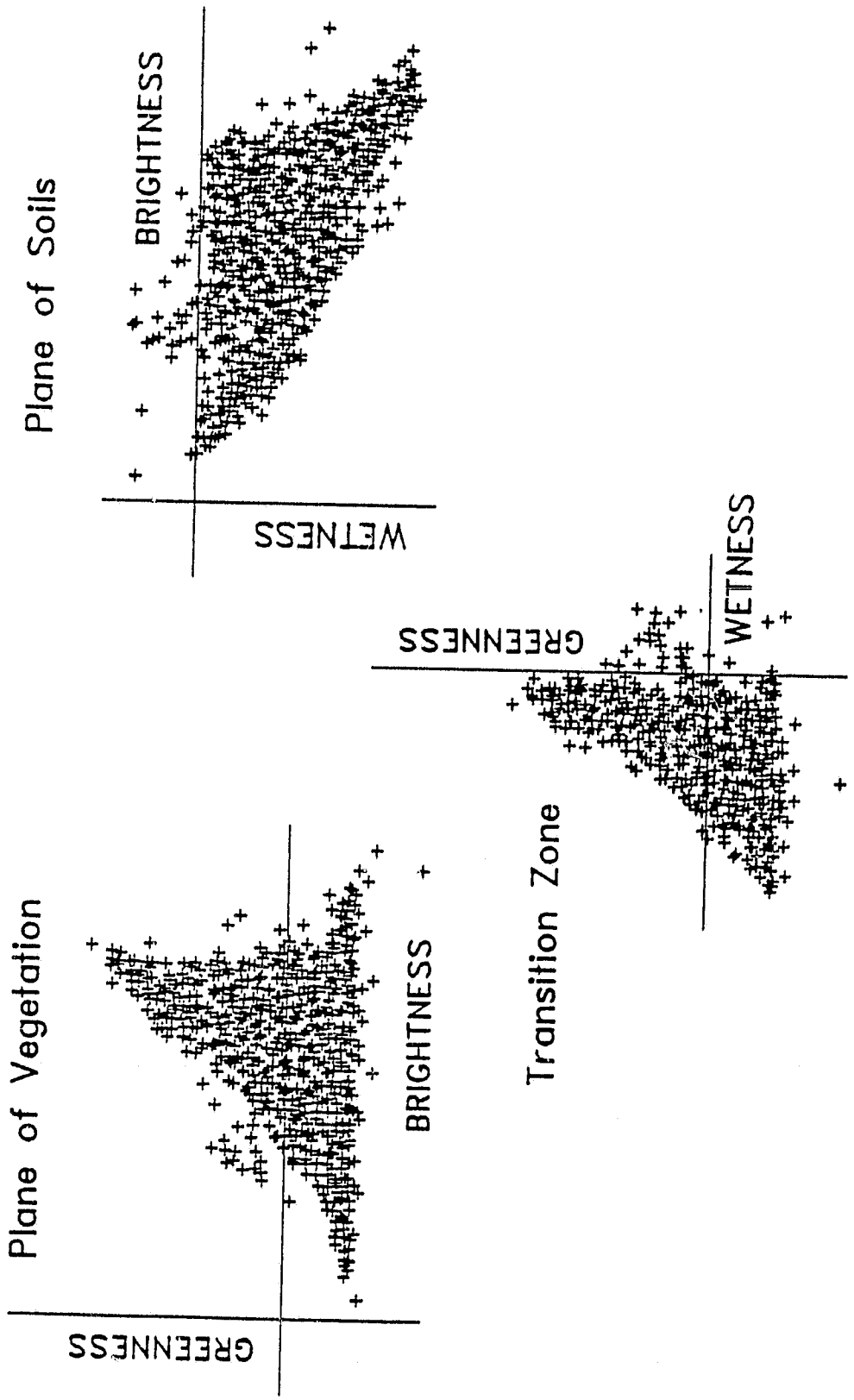

FIGURE 2.2. TM TASSELED CAP - ACTUAL DATA DISTRIBUTIONS FOR NORTH CAROLINA TEST SITE

TABLE 2.2. THEMATIC MAPPER TASSELED CAP COEFFICIENTS
(Present Configuration - see text for details)

	TM Band					
Feature	1	2	3	4	5	6
Brightness	.3037	.2793	.4743	.5585	.5082	.1863
Greenness	-.2848	-.2435	-.5436	.7243	.0840	-.1800
Wetness	.1509	.1973	.3279	.3406	-.7112	-.4572
Fourth	-.8242	.0849	.4392	-.0580	.2012	-.2768
Fifth	-.3280	.0549	.1075	.1855	-.4357	.8085
Sixth	.1084	-.9022	.4120	.0573	-.0251	.0238

characteristics of scene classes [2] can be most directly viewed and c) sensor data can be readily associated with physical scene characteristics. References 5 and 6 should be referred to for more detailed description and discussion of these results.

In order to better understand the projections of TM Tasseled Cap planes in the various band pairs, the North Carolina scene was used to define approximate plane coordinates, as illustrated in Figure 2.3. These coordinates, along with mean scene values of the fourth through sixth features, were then transformed back to TM band values, using the inverse of the TM Tasseled Cap matrix (Table 2.2). Figures 2.4 through 2.8 illustrate the resulting plane projections and actual data distributions in the TM band pairs. The Plane of Vegetation is depicted with solid lines, while the Plane of Soils is outlined using dashed lines. The Brightness direction, defined by the intersection of the two planes, always extends away from the origin (in a positive direction). The figures clearly show that, as with the MSS, each TM band carries some information, but none is directly aligned with the planes of data dispersion.

2.3 PHYSICAL EFFECTS ANALYSIS

Because of the similarity of the Plane of Vegetation view of the TM Tasseled Cap and the MSS data plane, many of the physical characteristics of scene classes expressed in that projection are already known. Of particular interest, therefore, are the physical scene properties principally responsible for variation in the third dimension of the TM data, as viewed in the Plane of Soils and Transition Zone views. In Reference 1, data variation in the Transition Zone is described as being primarily associated with changes in the relative mix of soil and vegetation in the sensor field of view, while variation in the Plane of Soils itself is suggested to be associated with soil moisture variation. Analyses in FY83 were directed at confirming this latter hypothesis.

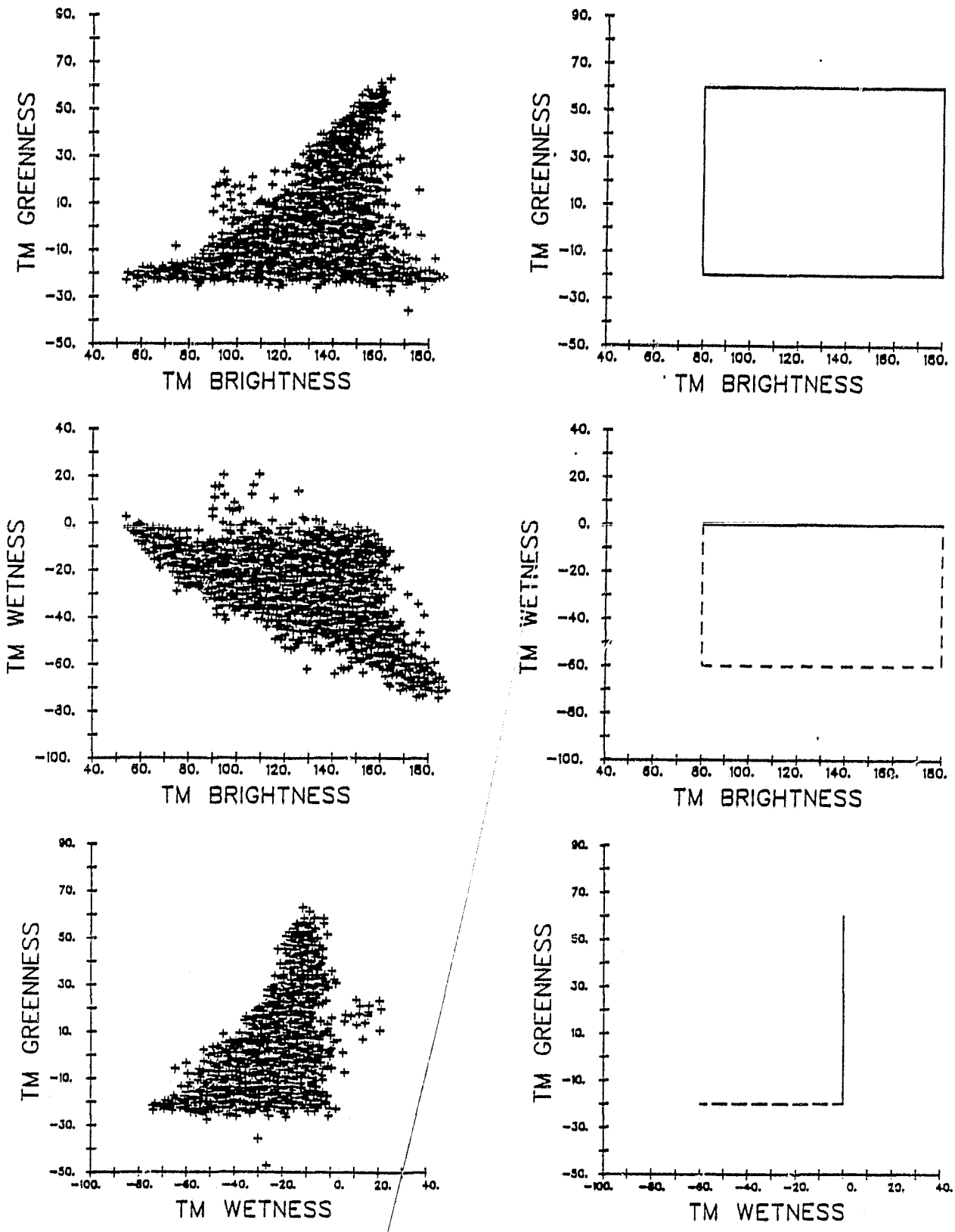

FIGURE 2.3. REPRESENTATION OF PLANES IN TM TASSELED CAP SPACE

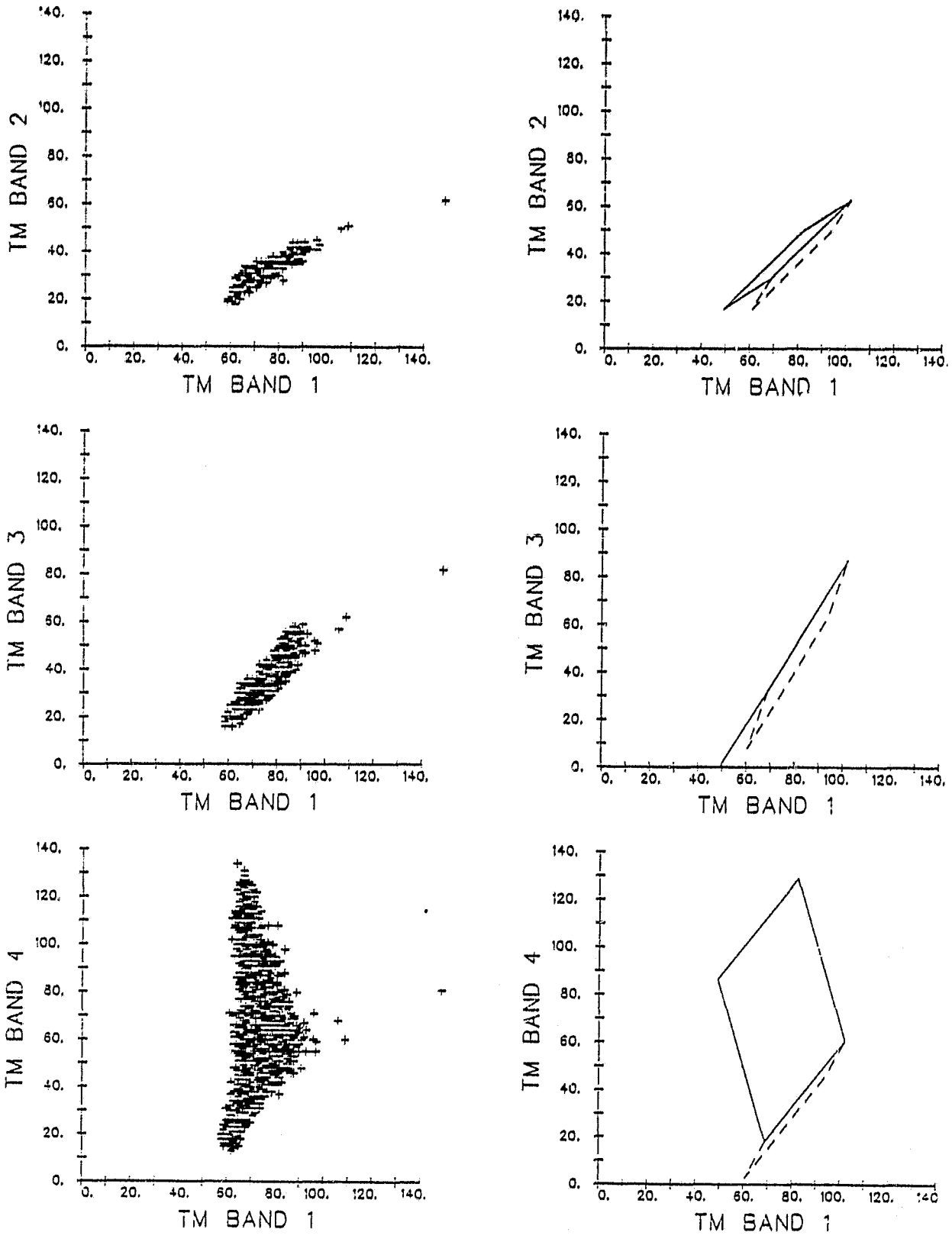

FIGURE 2.4. PROJECTION OF TM TASSELED CAP PLANES IN TM BAND PAIRS

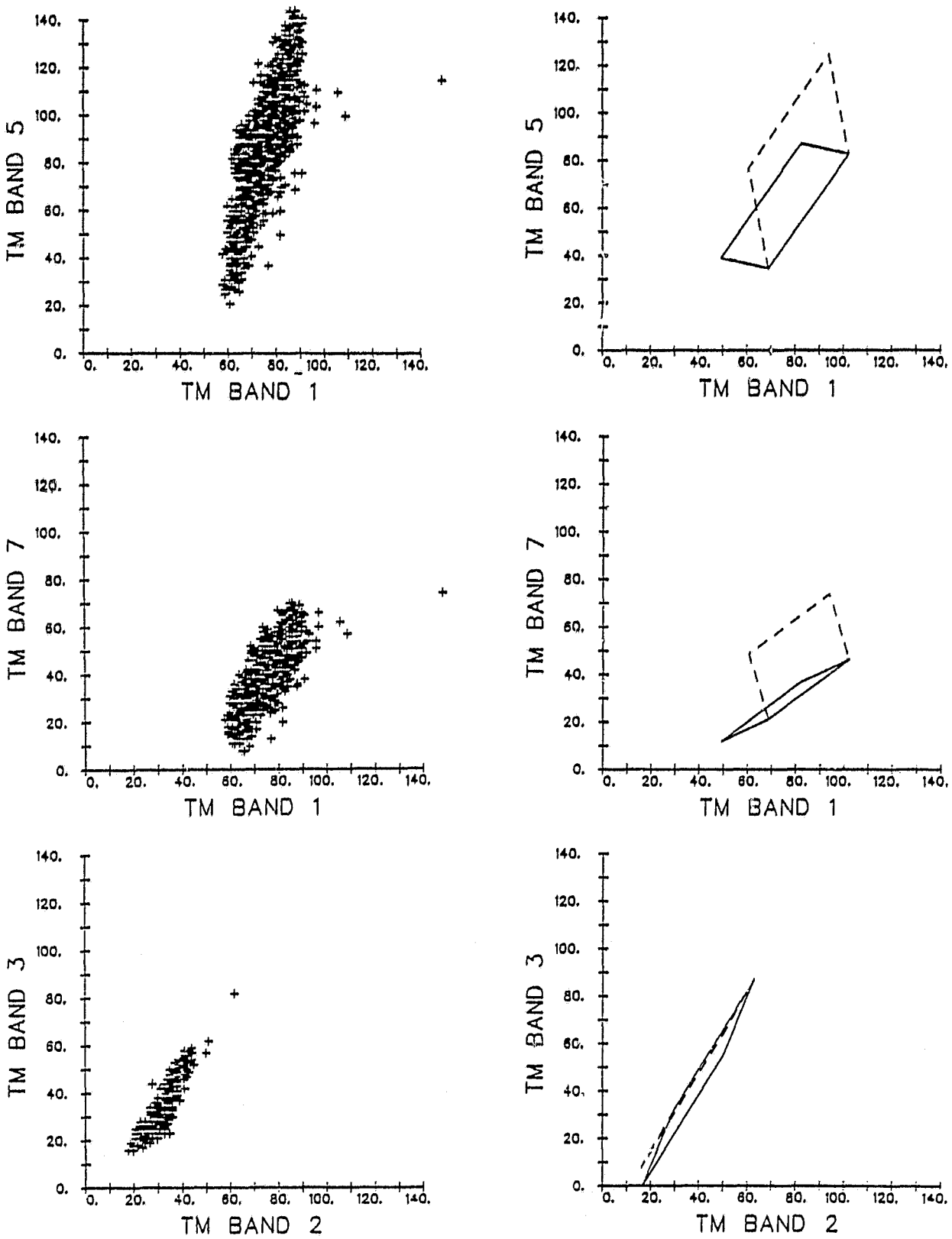

FIGURE 2.5. PROJECTION OF TM TASSELED CAP PLANES IN TM BAND PAIRS

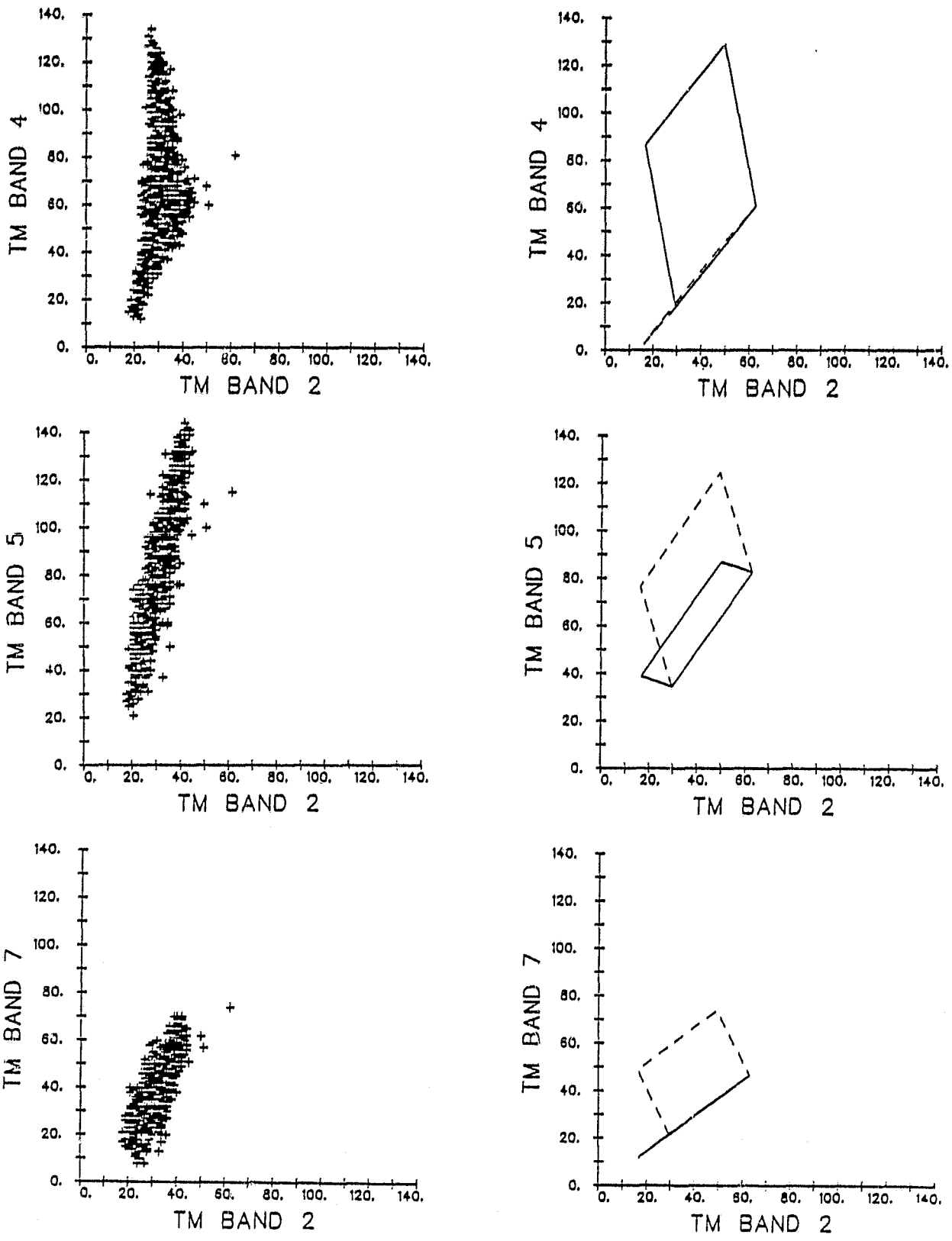

FIGURE 2.6. PROJECTION OF TM TASSELED CAP PLANES IN TM BAND PAIRS

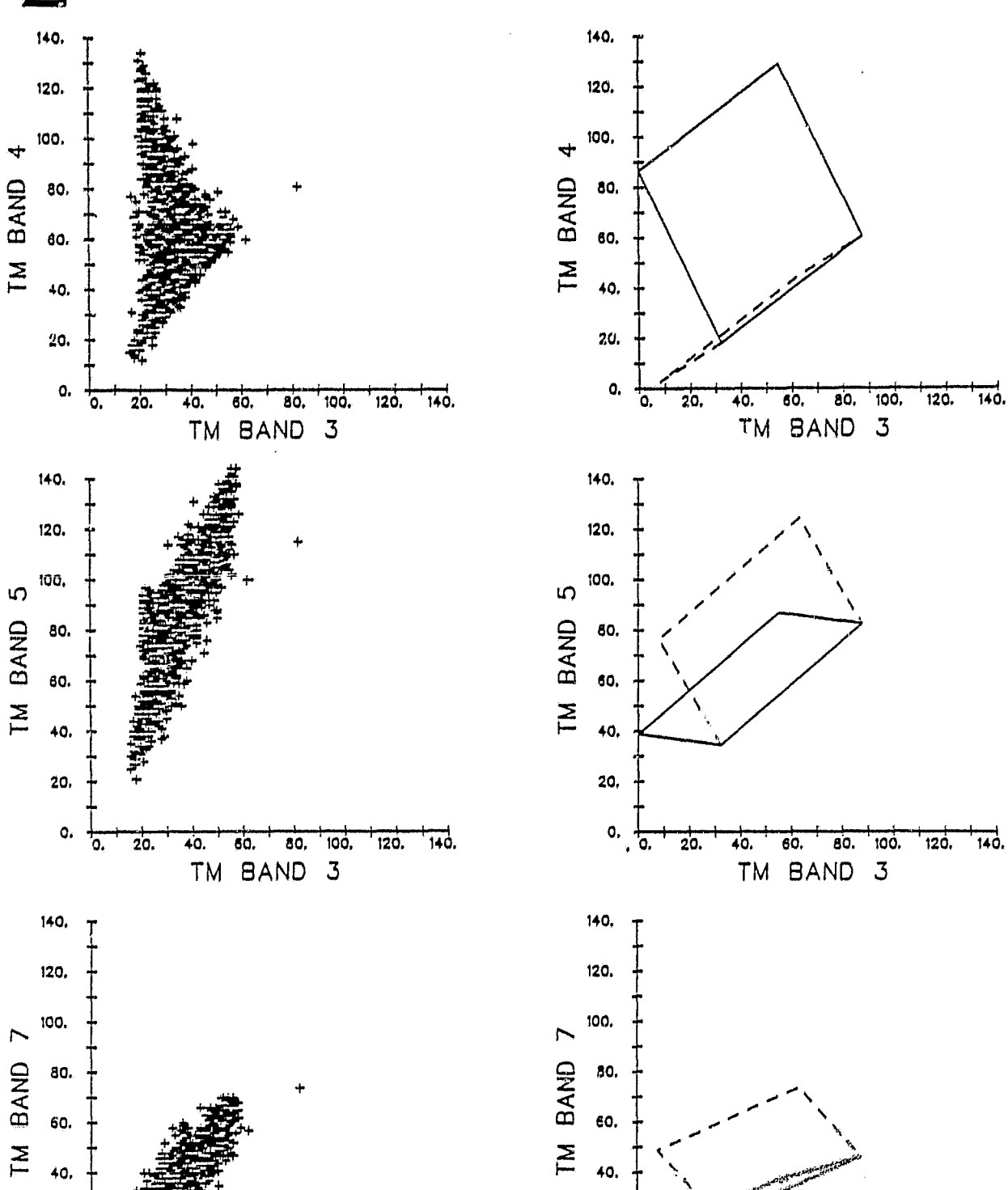

FIGURE 2.7. PROJECTION OF TM TASSELED CAP PLANES IN TM BAND PAIRS

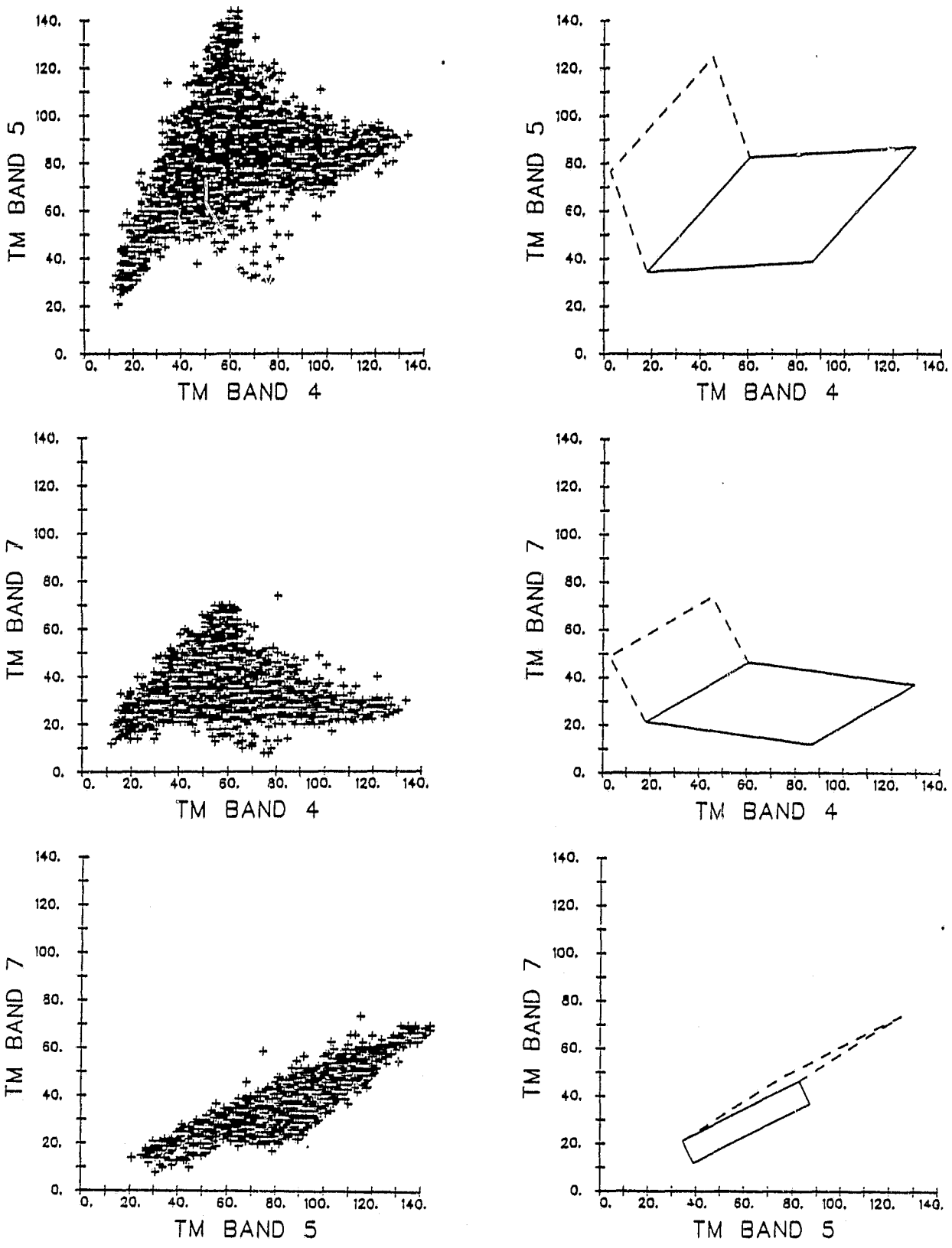

FIGURE 2.8. PROJECTION OF TM TASSELED CAP PLANES IN TM BAND PAIRS

Figure 2.9, which illustrates the simulated data in the Plane of Soils, demonstrates the apparent moisture-related signal variation. Three soil classes are present: moist lab soils (uniform moisture tension), field soil plots, and field plots of quarry sand. The latter two categories, as indicated in the figures, represent multiple measurements, through a growing season, of a few uniform plots. The observed variation within these two classes must therefore be associated not with some intrinsic soil property (particle size distribution, minerology, etc.) but with a soil condition. The condition perhaps most likely to vary over a several-month period is soil moisture.

A further test of this hypothesis was carried out using the lab-measured soils. In most cases, two samples of a particular soil series were included in the data set. The technique by which the two were selected resulted in the possibiliity of substantial variation in soil properties and/or conditions between them [7]. By selecting soil series pairs which varied significantly in a particular soil property but little in other properties, the effect of a single soil property could be evaluated. Based on Stoner's work [7] seven properties were selected for analysis: fine sand %, medium sand %, clay %, moisture % by weight, cation exchange capacity, iron oxide content and organic carbon content. The effect of changes in these properties was determined, in the Plane of Soils, for five to ten series pairs selected as previously described. Figures 2.10 and 2.11 illustrate sample results for relative change in moisture content and relative change in clay content. Only moisture percent by weight showed a clear and consistent effect, supporting the previous hypothesis.

It should be remembered that the soil samples, while varying substantially in moisture percent by weight, were measured at a uniform moisture tension. Although moisture tension is probably nearer to the measurement actually desired for biological productivity analysis, for example, it is the actual amount of water in the soil which affects the reflectance of that soil.

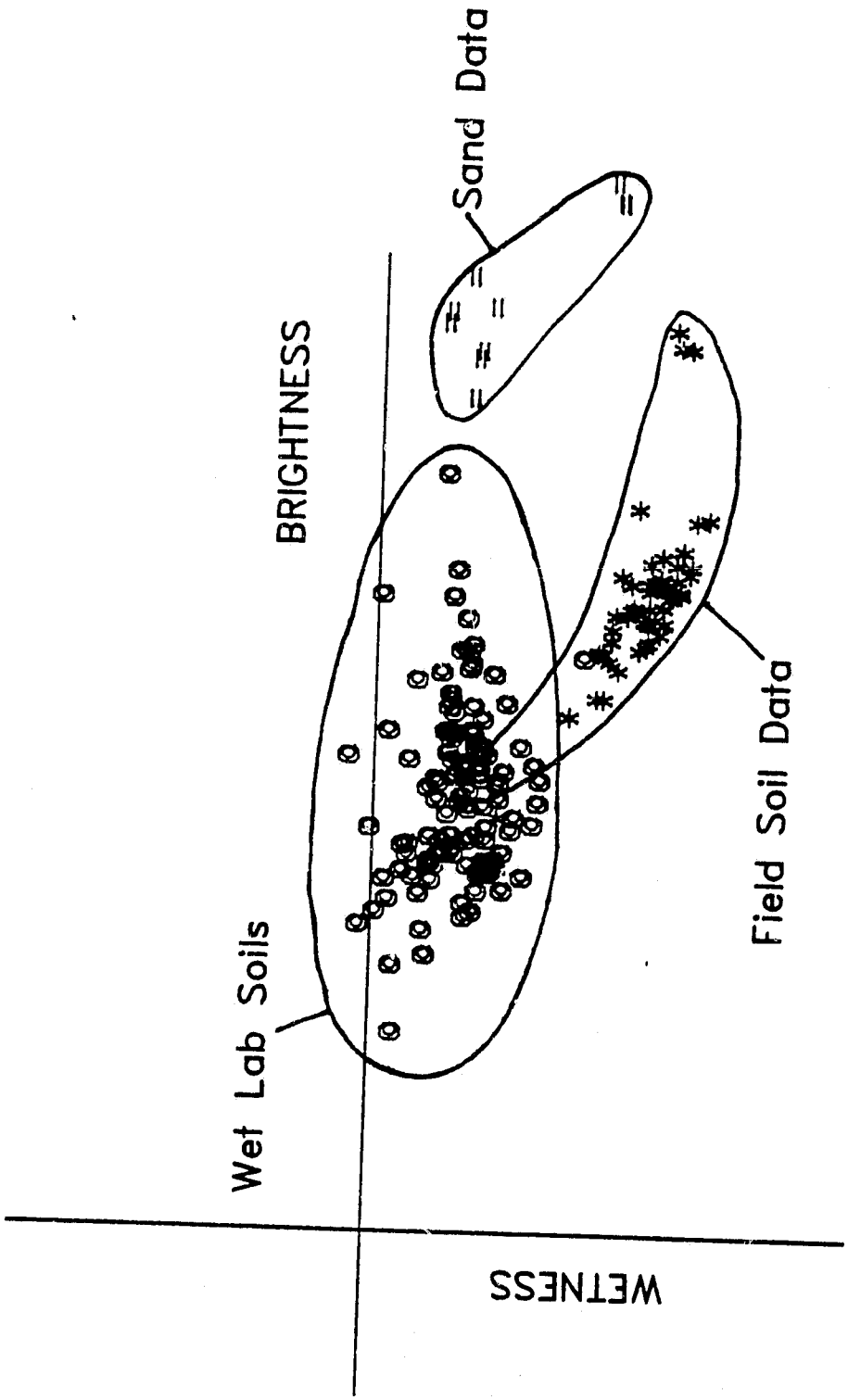

FIGURE 2.9. SOILS IN THE TM TASSELED CAP PLANE OF SOILS (SIMULATED DATA)

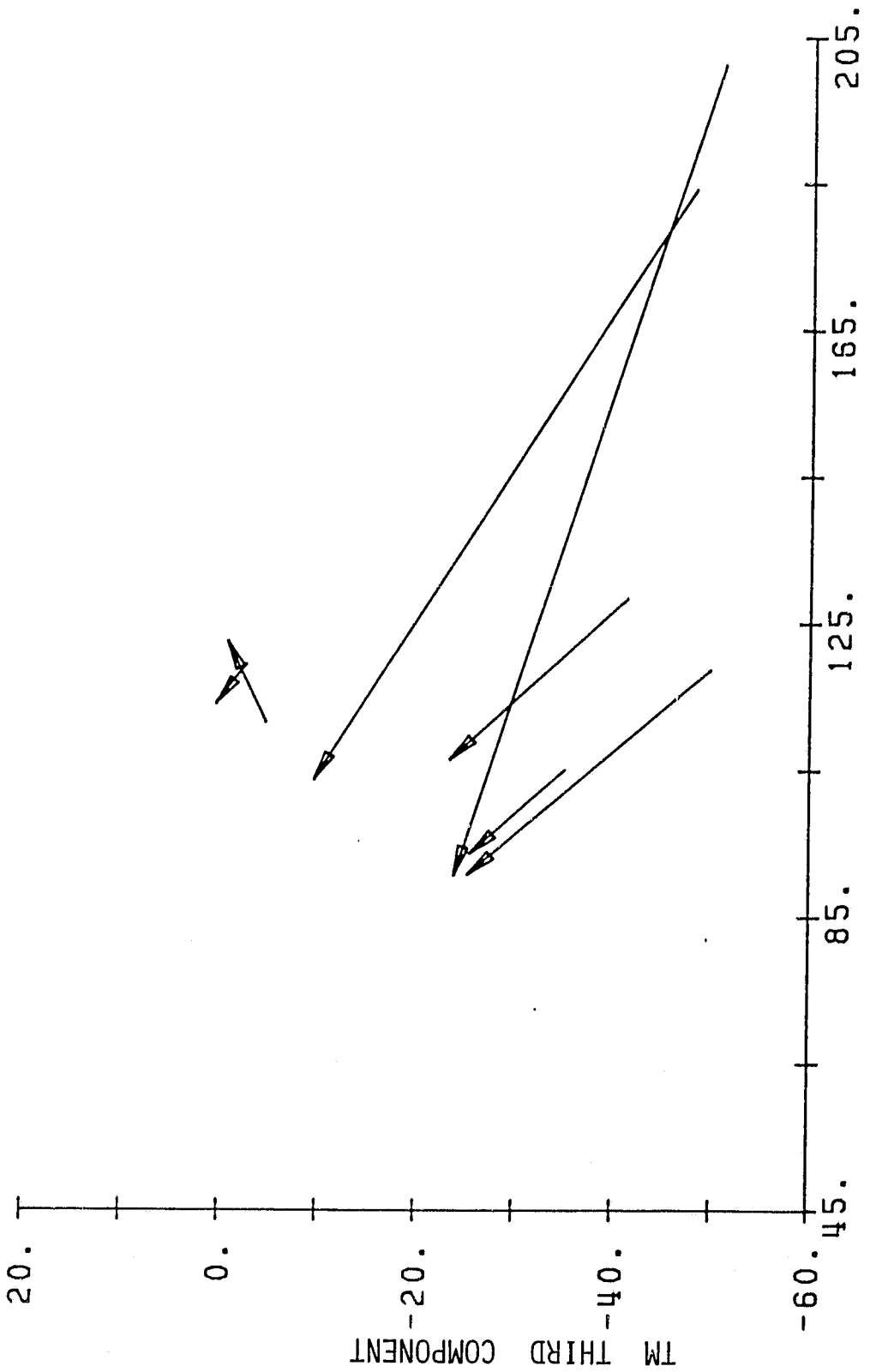

FIGURE 2.10. MAGNITUDE AND DIRECTION OF SPECTRAL CHANGE IN RESPONSE TO CHANGE IN MOISTURE % BY WEIGHT

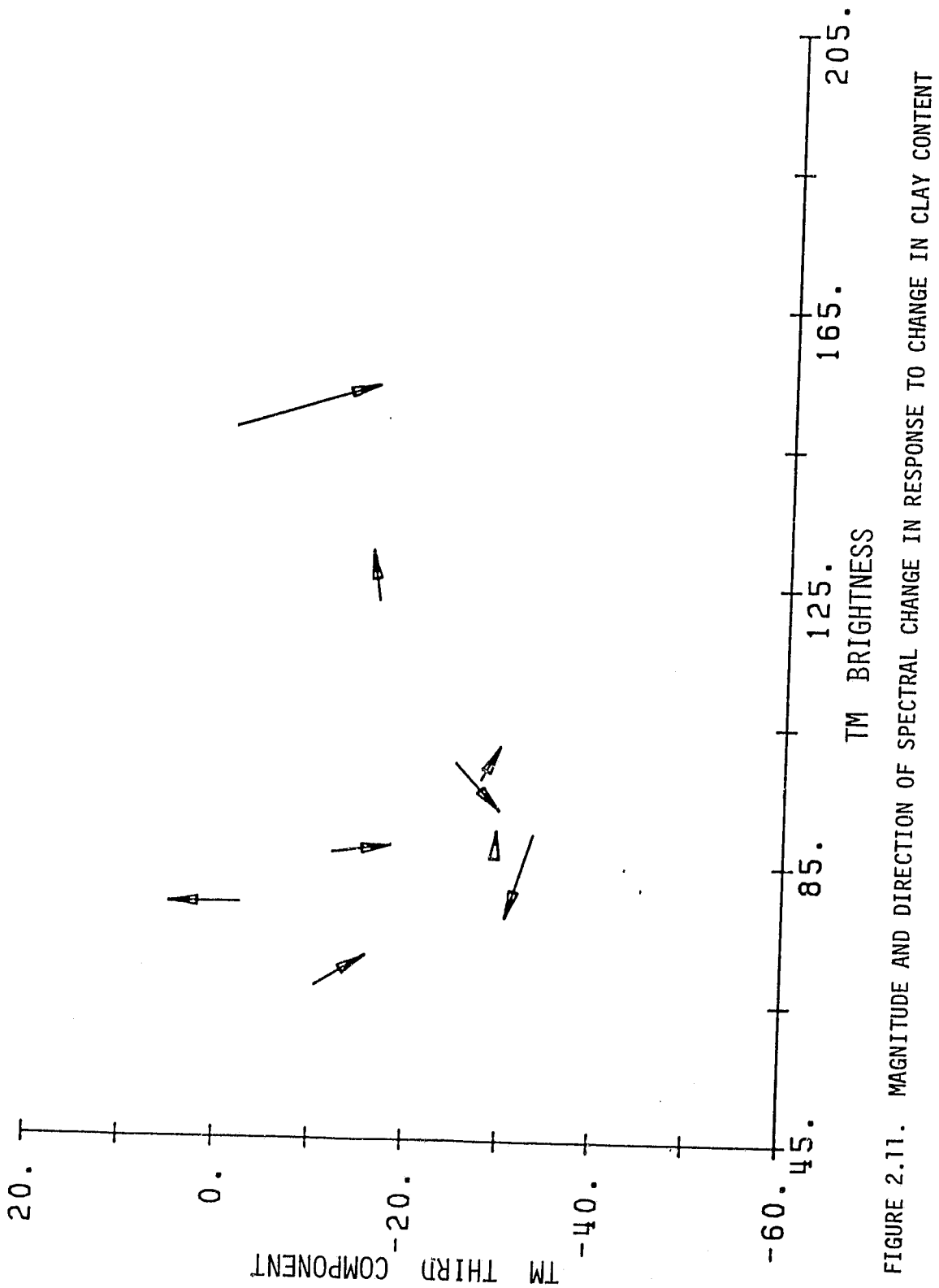

FIGURE 2.11. MAGNITUDE AND DIRECTION OF SPECTRAL CHANGE IN RESPONSE TO CHANGE IN CLAY CONTENT

By drawing in classes from the actual TM data sets, a direction of moisture variation can be defined, as shown in Figure 2.12. Adding to the wet and dry soils described above water as the ultimately wet material and concrete as an extremely dry material, a clear moisture direction emerges. Based on these results, the name "Wetness" was assigned to the third TM Tasseled Cap feature. Clearly moisture variation has a Wetness and a Brightness component. However, relative differences in Brightness need not be related to moisture variation, but rather might reflect differences in particle size distribution or other properties. Variation in the Wetness direction, on the other hand, appears to be more reliable as an absolute moisture indicator, even between soil classes of substantially different reflectance (as between the field soil and sand classes in Figure 2.9).

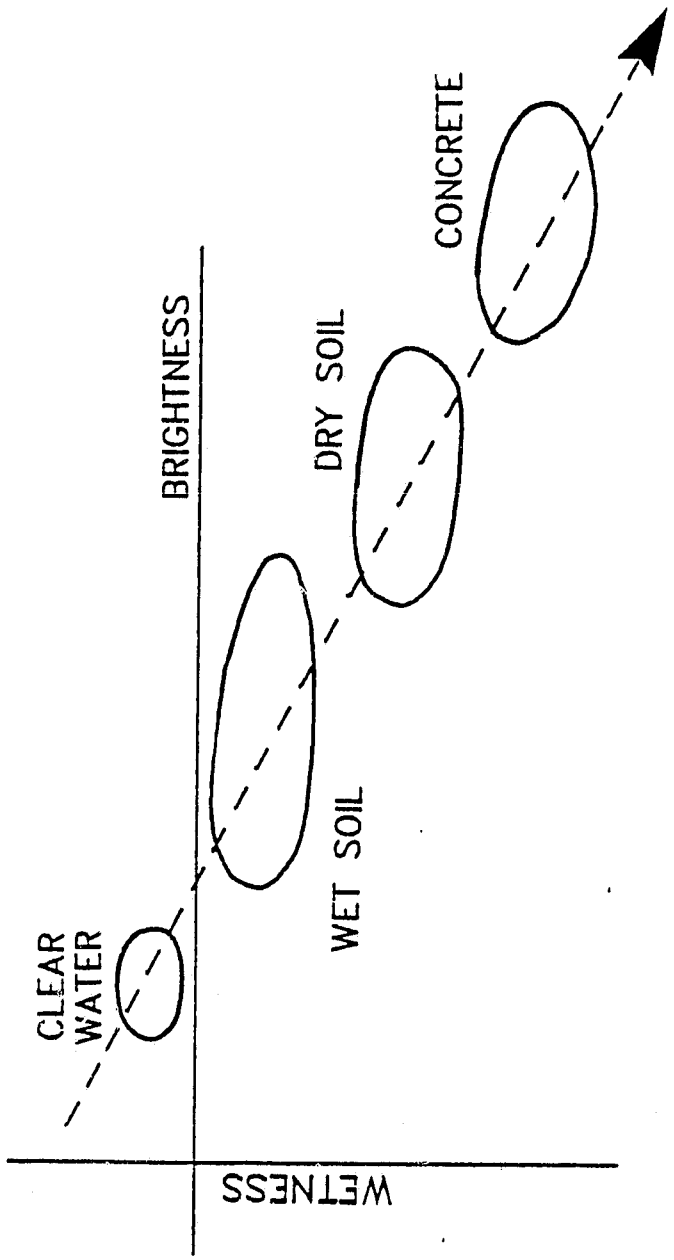

FIGURE 2.12. DIRECTION OF SOIL MOISTURE VARIATION IN PLANE OF SOILS

3.0
THEMATIC MAPPER EXTERNAL EFFECTS ANALYSIS

Monitoring trends or changes in the areal extent of particular cover types and, in most cases, distinguishing between vegetative cover types requires the use of multitemporal sensor data. Effect use of multitemporal data, in turn, requires that the effects of external conditions such as atmospheric haze and sun zenith angle be taken into account. Understanding and correction of these effects is thus of considerable importance to many of the current and intended uses of satellite sensor data.

Both because of the complex nature of these effects and because of the difficulty of acquiring an adequate set of actual sensor data, simulation is the best means for obtaining initial understanding of external effects on TM data. Section 3.1 describes the two atmospheric models to be used, and compares their results for a common set of conditions. Section 3.2 describes analysis of the output from one of those models, while Section 3.3 presents the derivation of a haze diagnostic feature for the simulated TM data.

3.1 COMPARISON OF ATMOSPHERIC MODELS

The ideal simulation model would combine precision with flexibility, allowing the user to examine accurate representations of a wide range of states or conditions. In the case of readily-available visible and near-infrared atmospheric models, no single model fulfills both of these requirements. As a result, a series of comparisons of a set of models, described below, was undertaken for the purpose of understanding their relative accuracies. Understanding how the models perform under comparable conditions may allow the use of the more flexible but less accurate models to expand the range of conditions available from the more precise models.

3.1.1 MODEL DESCRIPTIONS

The Dave model [8] is considered by many to be the current state of the art in atmospheric modeling for the visible and near-infrared wavelengths. Based on a numerical solution of the Spherical Harmonics Approximation [9,10] to the radiative transfer equation, this model assumes a horizontally homogeneous plane parallel atmosphere with Lambertian target and background reflectors. Calculations are made for 15 basic atmospheric layers, taking into account target and background reflectance, total optical thickness, gaseous absorption, viewing geometry and air pressure. This model would be the logical choice for any ground-to-satellite simulation except for one major drawback - only five data sets are publicly available, and of these only two are for complete atmospheres with aerosol distributions typically found over large land masses. Thus with the available data, one can achieve only a limited view of what is in fact a very complex function. For this reason, three other models were compared to the Dave model: the Turner Double Delta Approximation [9,10], an iterated solution of the Eddington Approximation [10,11] and the Quasi-Single Scattering (QSS) Approximation [10,11]. These models were selected based on their availability, as well as on their ability to compute results for many sets of atmospheric parameters.

Turner's Double Delta model is an interated approximation derived by substituting into the radiative transfer equation a phase function that decomposes the scattered radiation into forward and backward components. This model (indeed, each of the models used) makes the same plane parallel and Lambertian assumptions as the Dave model. However, the atmosphere is only divided into two layers - above and below the observation point. For satellite sensors (above the atmosphere), this means a single layer atmosphere. The calculations in the Turner model include components for target and background reflectance, total optical thickness, gaseous absorption, viewing geometry and anisotropy.

The iterated solution of the Eddington Approximation, in contrast to Turner's model, averages radiance over all space rather than hemispheres. The form of this solution available to this task also assumes no contribution from background reflectance and no gaseous absorption.

The QSS model, in addition to the plane parallel and Lambertian assumptions, assumes that any radiation is scattered only once. In addition, the form available assumes no contribution from background reflectance.

3.1.2 APPROACH

Two sets of atmospheric parameters were derived by extracting the relevant information from the Dave data sets corresponding to clear and hazy conditions over a large continental land mass (Models 3 and 4, respectively). Values for atmospheric pressure at ground level, total optical thickness (Figure 3.1) and single scattering albedo (Figure 3.2) were obtained in this way. Rayleigh optical thickness and anisotropy were computed from the atmospheric pressure at ground level [9].

The normalized scattering phase functions used by Dave were not retrievable from his data sets. Hence, the phase function from the Turner model [10] corresponding to particle distribution over large continental land masses was used in the three alternate models. The literature [8,10] suggests that the two functions were derived in the same way and therefore should be similar if not identical.

The reflectance data were derived from a large data base of field-collected spectra [12] by individually averaging the values for six representative soil types and for wheat in ten stages of vegetative development. Figure 3.3 shows the soil spectra and a sample spanning the range of the wheat spectra.

Initially all four models were run under the assumption that target reflectance equaled background reflectance and with a solar

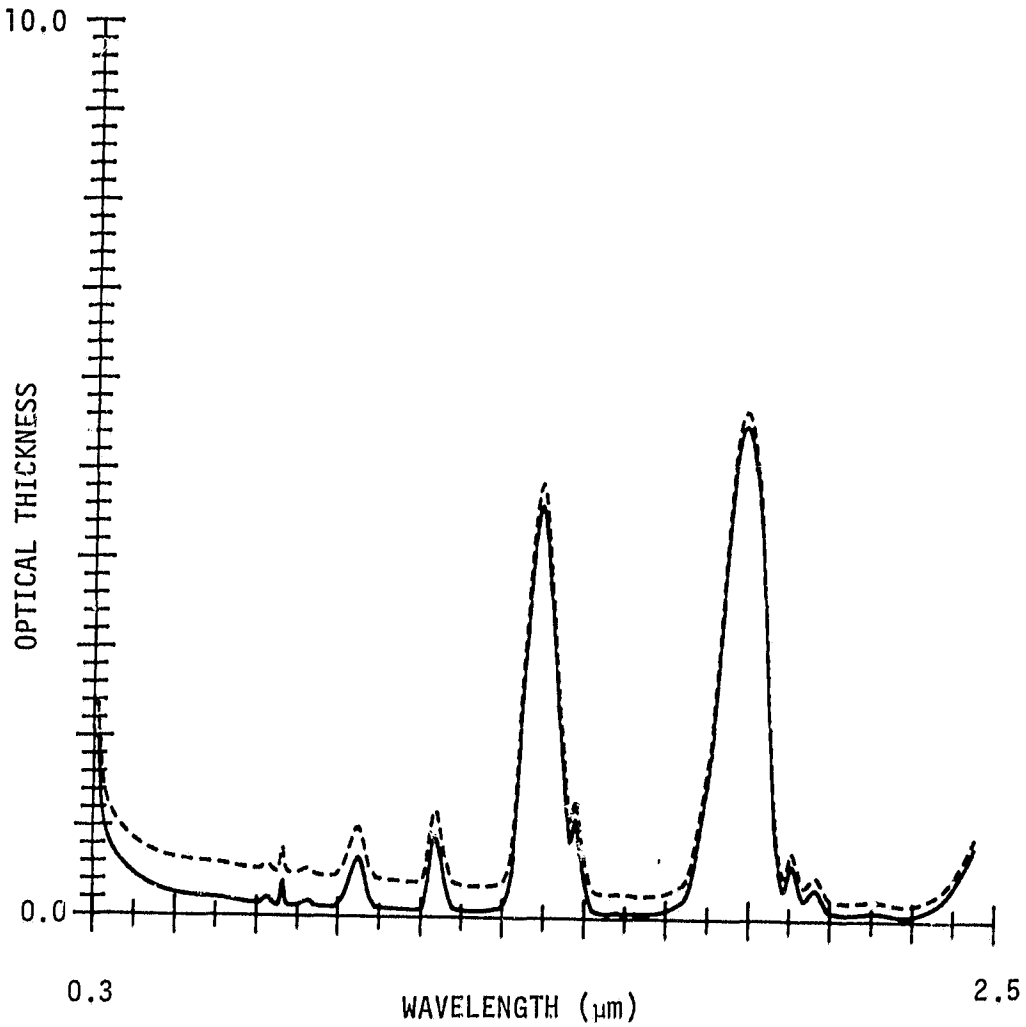

FIGURE 3.1. OPTICAL THICKNESS FOR TEST CONDITIONS
KEY: —— = clear atmosphere, --- = hazy atmosphere

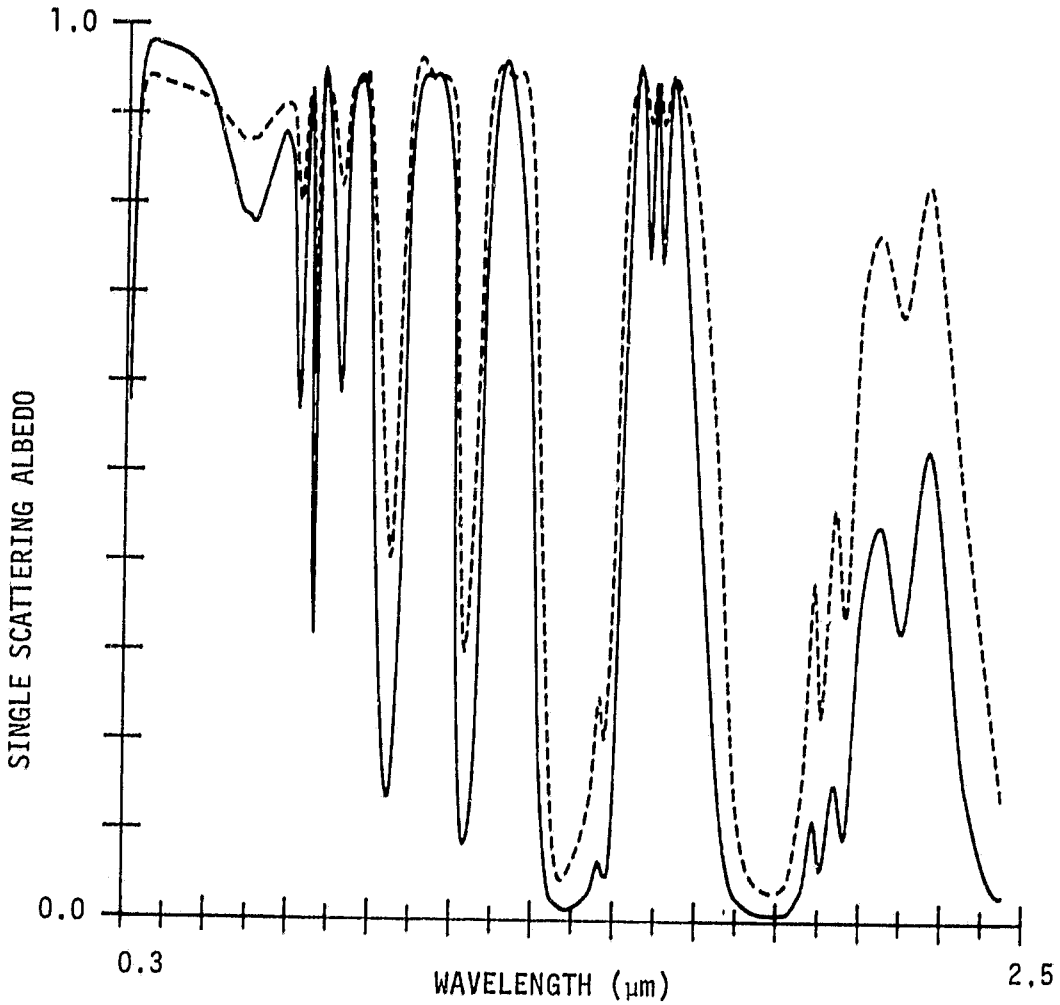

FIGURE 3.2. SINGLE SCATTERING ALBEDO FOR TEST CONDITIONS
KEY: —— = clear atmosphere, --- = hazy atmosphere

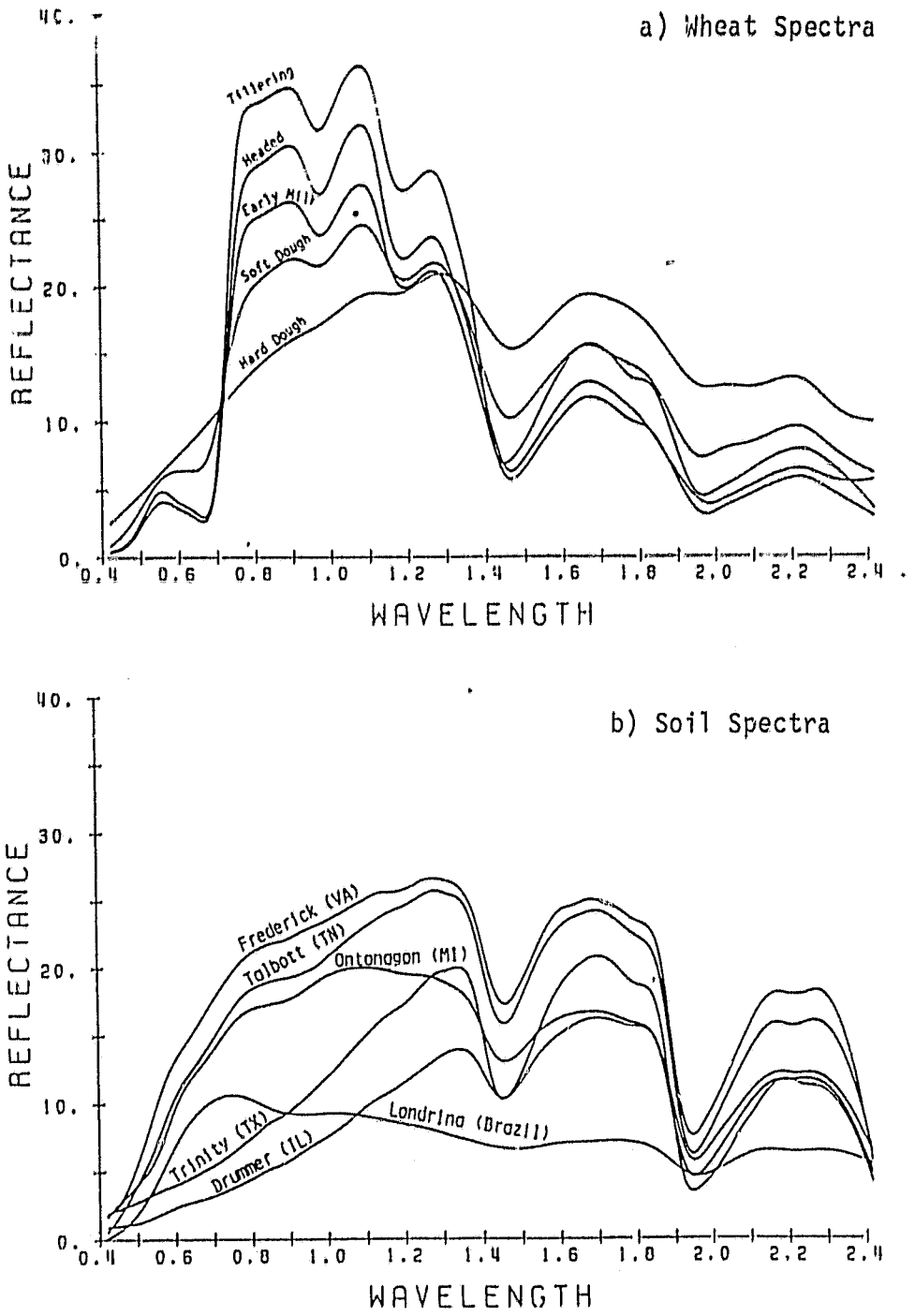

FIGURE 3.3. AVERAGED REFLECTANCE SPECTRA USED IN ANALYSIS

zenith angle of 45 degrees. The Dave and Turner models were also run with a background reflectance spectrum obtained by averaging the sample soil and wheat spectra. Solar zenith angles of 45 and 30 degrees were used for these runs.

3.1.3 RESULTS

Figures 3.4 and 3.5 shows the target, path and total radiances predicted by the four models (as a function of wavelength) for a representative wheat spectrum assuming infinite field size (background reflectance equal to target reflectance). Target radiance is defined as that portion of the total radiance which is due solely to the energy reflected by the target. All other predicted radiance is combined into path radiance.

As expected, the models are near agreement in the clear case (little atmospheric contribution), and show more divergence in the hazy case. The Turner and Eddington models predict target radiances very close to those predicted by the Dave model. The QSS model overestimates target radiance relative to Dave, a result attributable to the fact that the QSS model used calculates target radiance using diffuse transmittance rather than direct transmittance.

It is in predicting radiance not due directly to the target that the models vary the most. In comparison to Dave, Turner consistently underestimates the effects of path radiance in all wavelengths. The Eddington approximation does much better in the lower wavelengths than the Turner model. However, it does not contain a component for background radiance and hence underestimates path radiance in the 0.7 to 0.9 μm range. This is also a problem with the QSS model. The overestimation in the 1.8 to 1.9 μm band by Eddington occurs because the available form ignores absorption.

The effects of changing the background assumption and solar zenith angle are shown in Figure 3.6. Here, the difference between predicted total radiances for clear and hazy atmosphere is shown for three sets

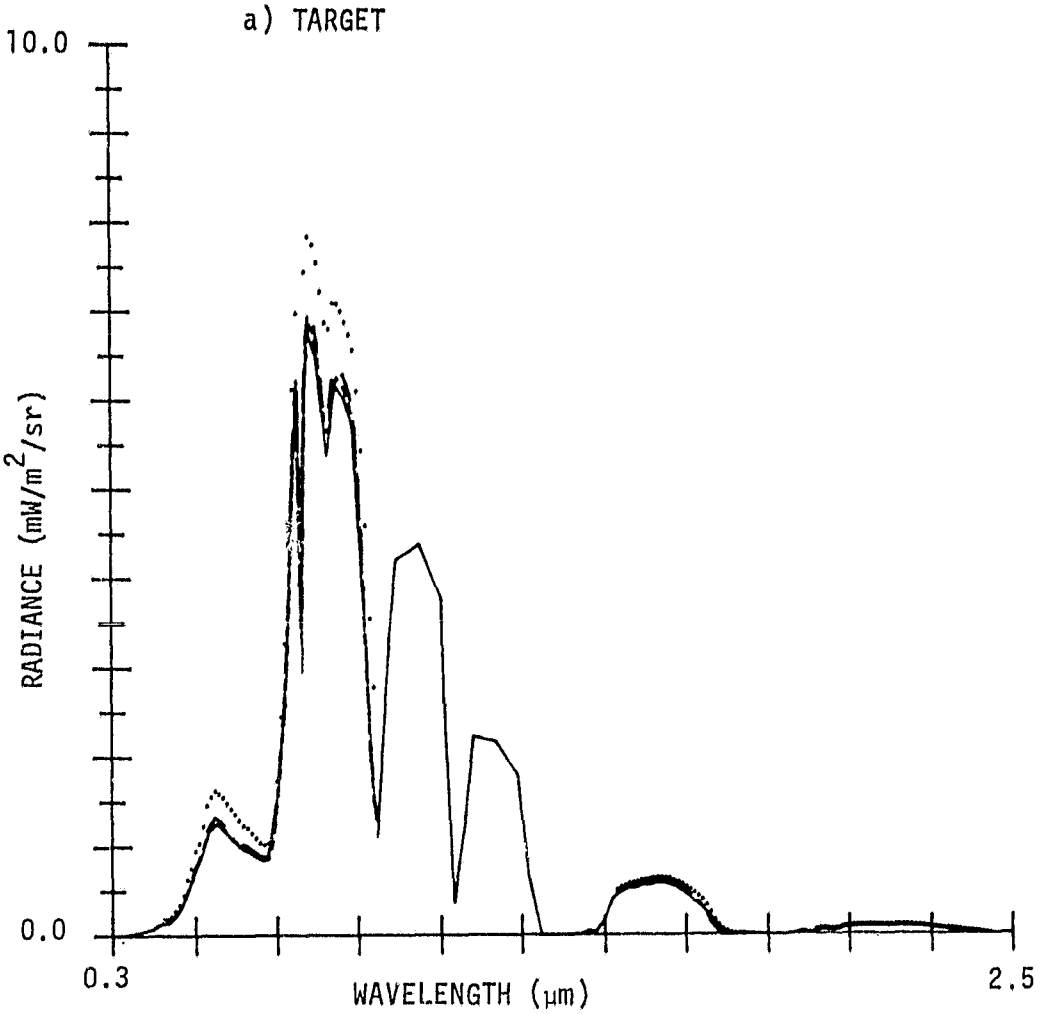

FIGURE 3.4. MODEL RESULTS FOR CLEAR ATMOSPHERE, 45^{o} SUN, INFINITE FIELD SIZE, WHEAT SPECTRUM #2

KEY: —— = Dave, — — = Turner, --- = Eddington, ... = QSS

b) PATH

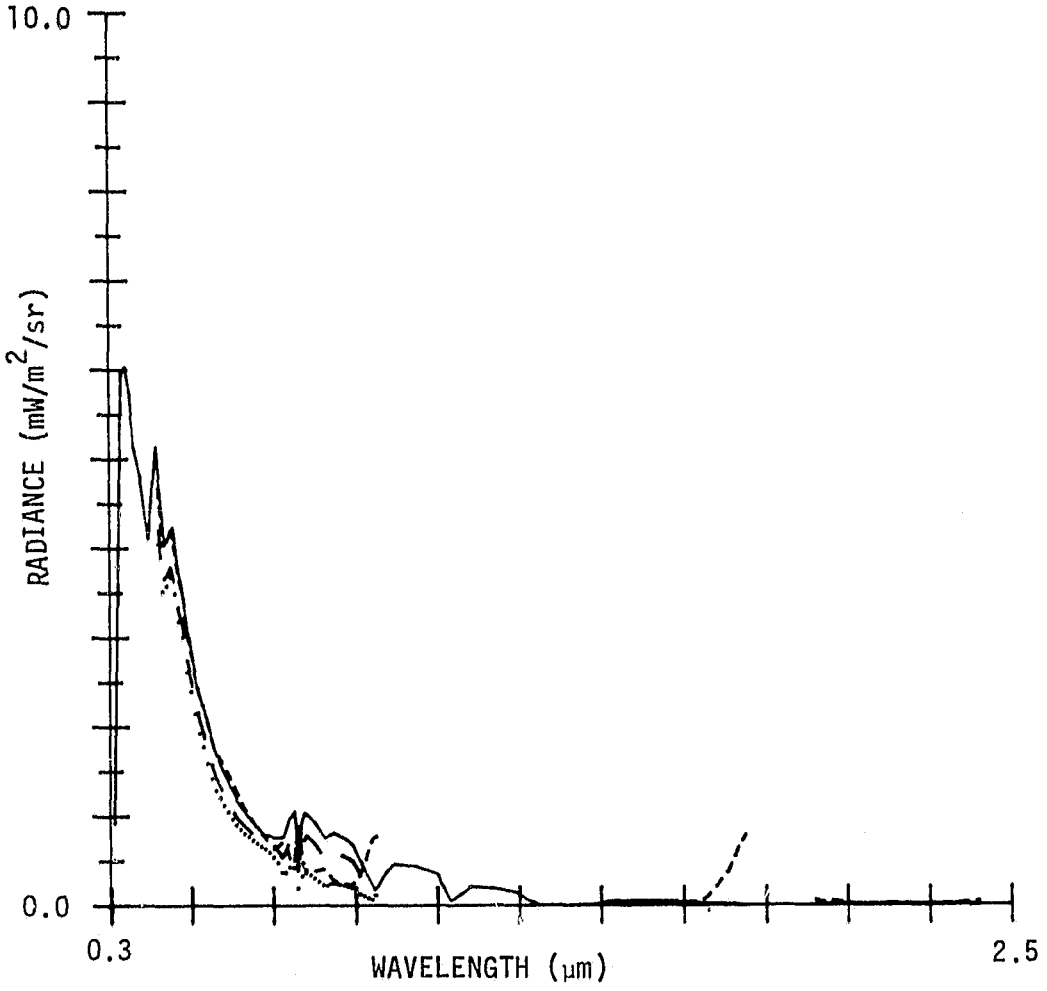

FIGURE 3.4. MODEL RESULTS FOR CLEAR ATMOSPHERE, 45^o SUN, INFINITE FIELD SIZE, WHEAT SPECTRUM #2 (Continued)

c) TOTAL

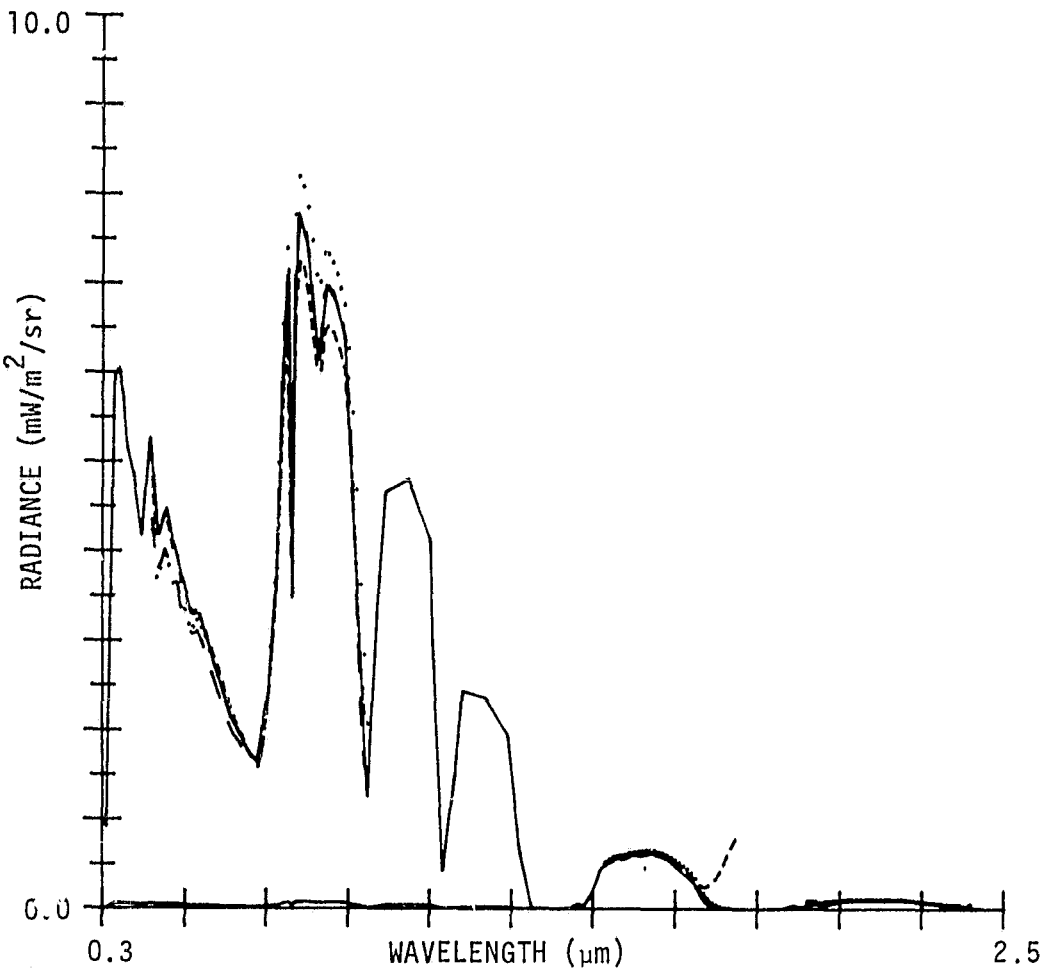

FIGURE 3.4. MODEL RESULTS FOR CLEAR ATMOSPHERE, 45^o SUN, INFINITE FIELD SIZE, WHEAT SPECTRUM #2 (Continued)

a) TARGET

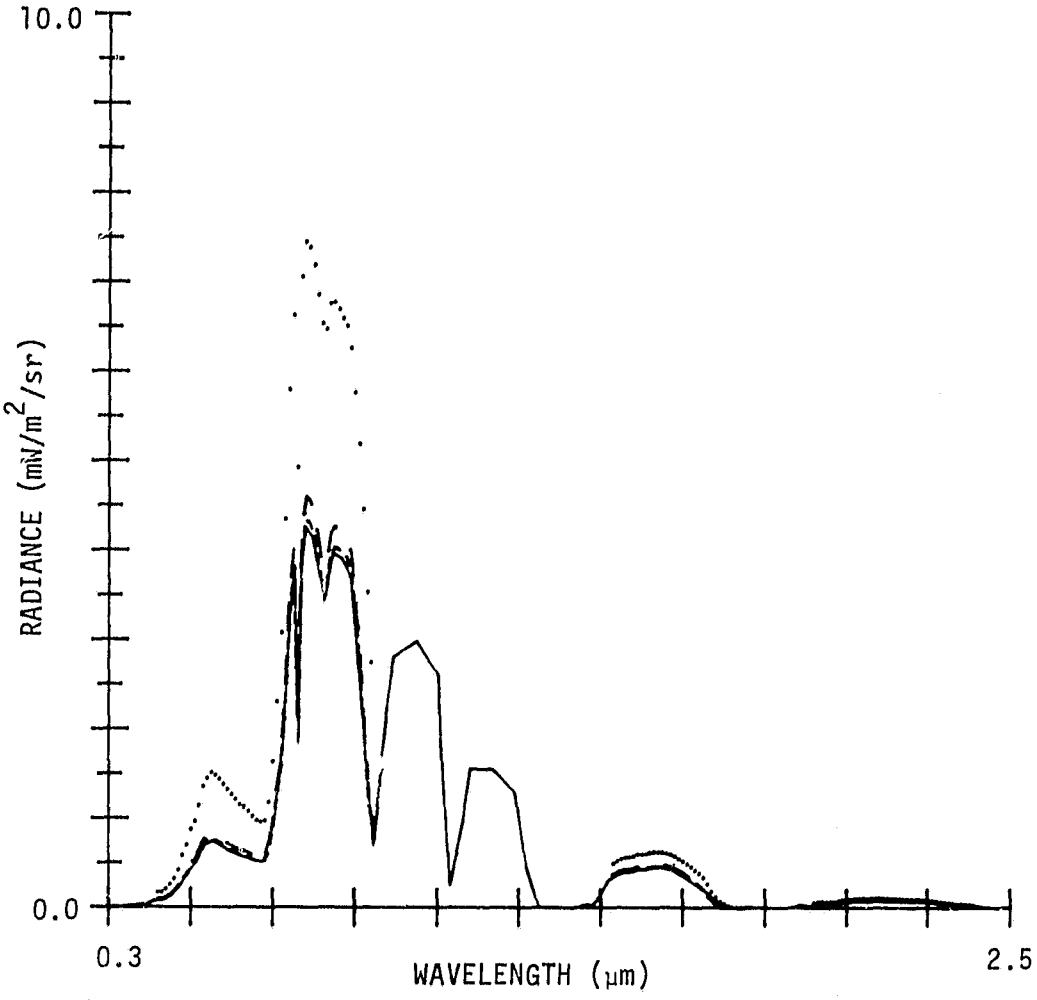

FIGURE 3.5. MODEL RESULTS FOR HAZY ATMOSPHERE, 45^o SUN, INFINITIE FIELD SIZE, WHEAT SPECTRUM #2

KEY: —— = Dave, — — = Turner, --- = Eddington, ... = QSS

b) PATH

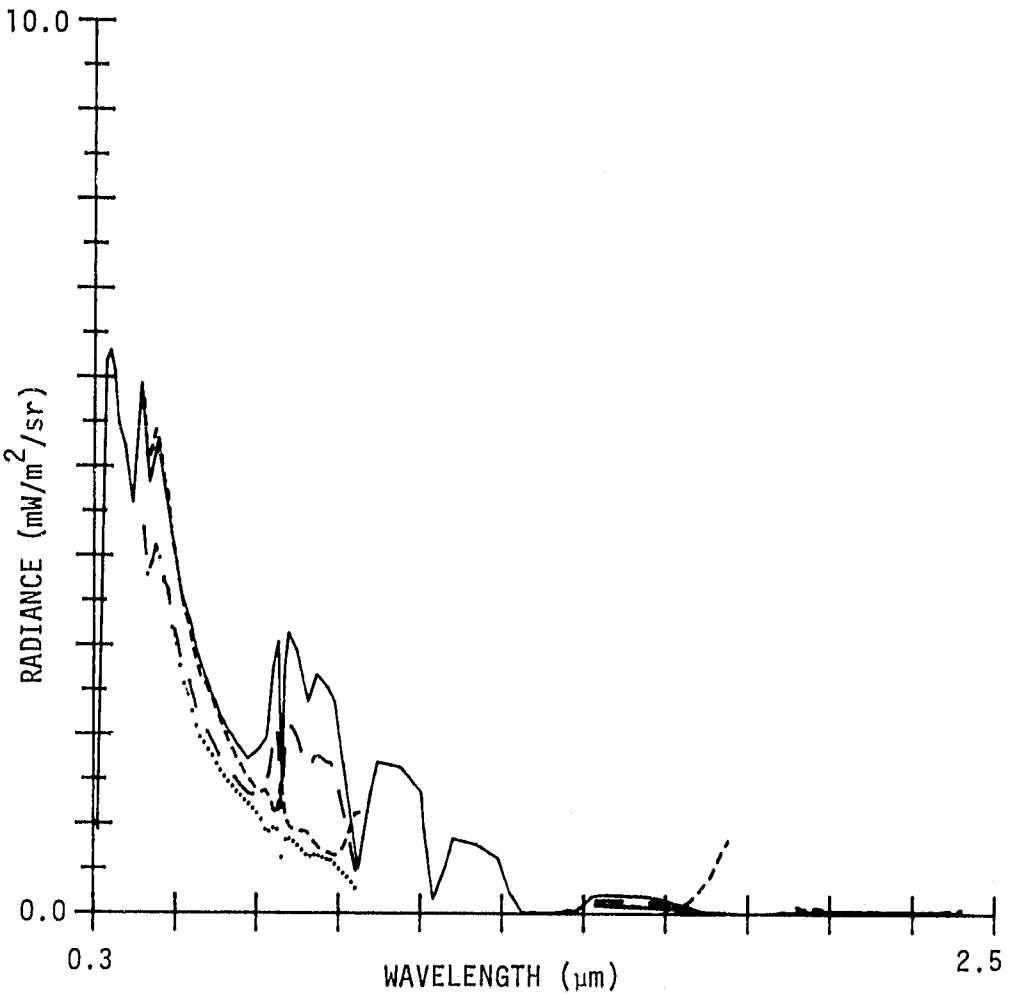

FIGURE 3.5. MODEL RESULTS FOR HAZY ATMOSPHERE, 45^o SUN, INFINITE FIELD SIZE, WHEAT SPECTRUM #2 (Continued)

c) TOTAL

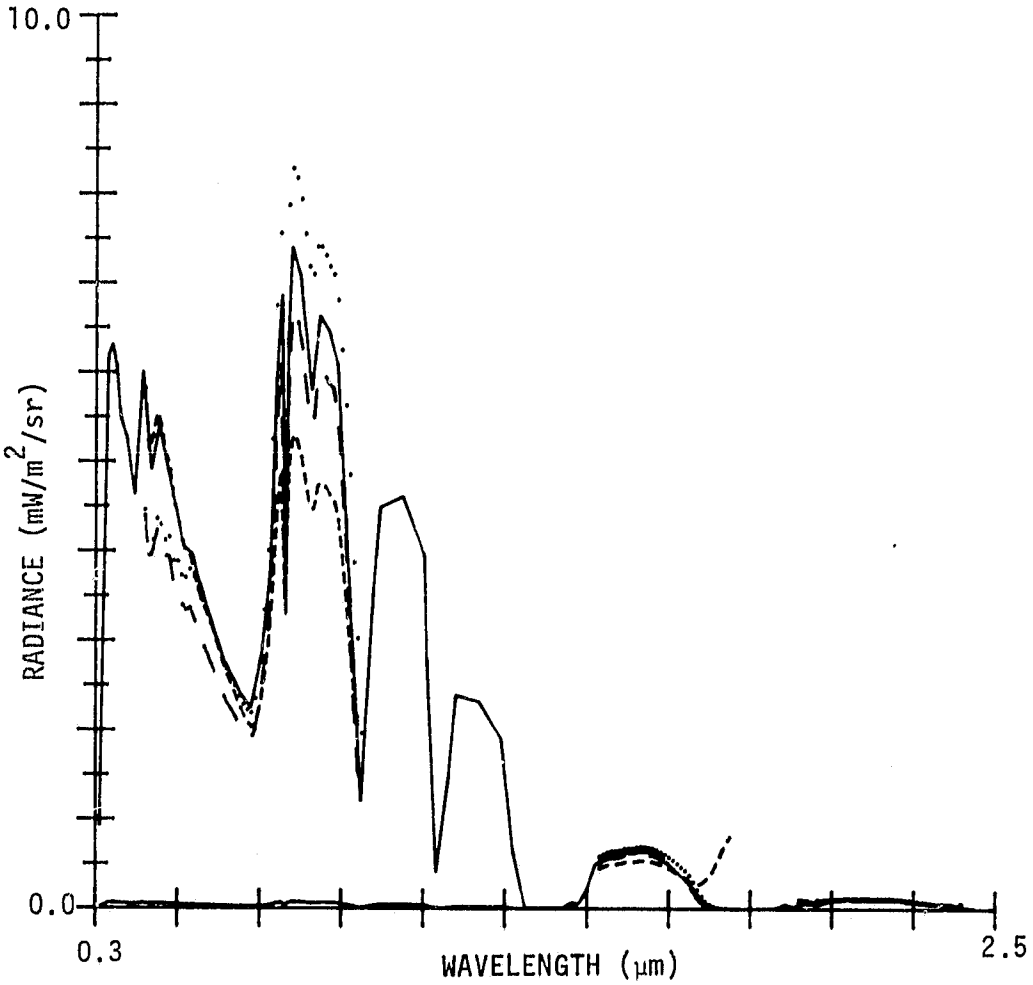

FIGURE 3.5. MODEL RESULTS FOR HAZY ATMOSPHERE, 45^o SUN, INFINITE FIELD SIZE, WHEAT SPECTRUM #2 (Continued)

a) Infinite Field Size, 45° Sun

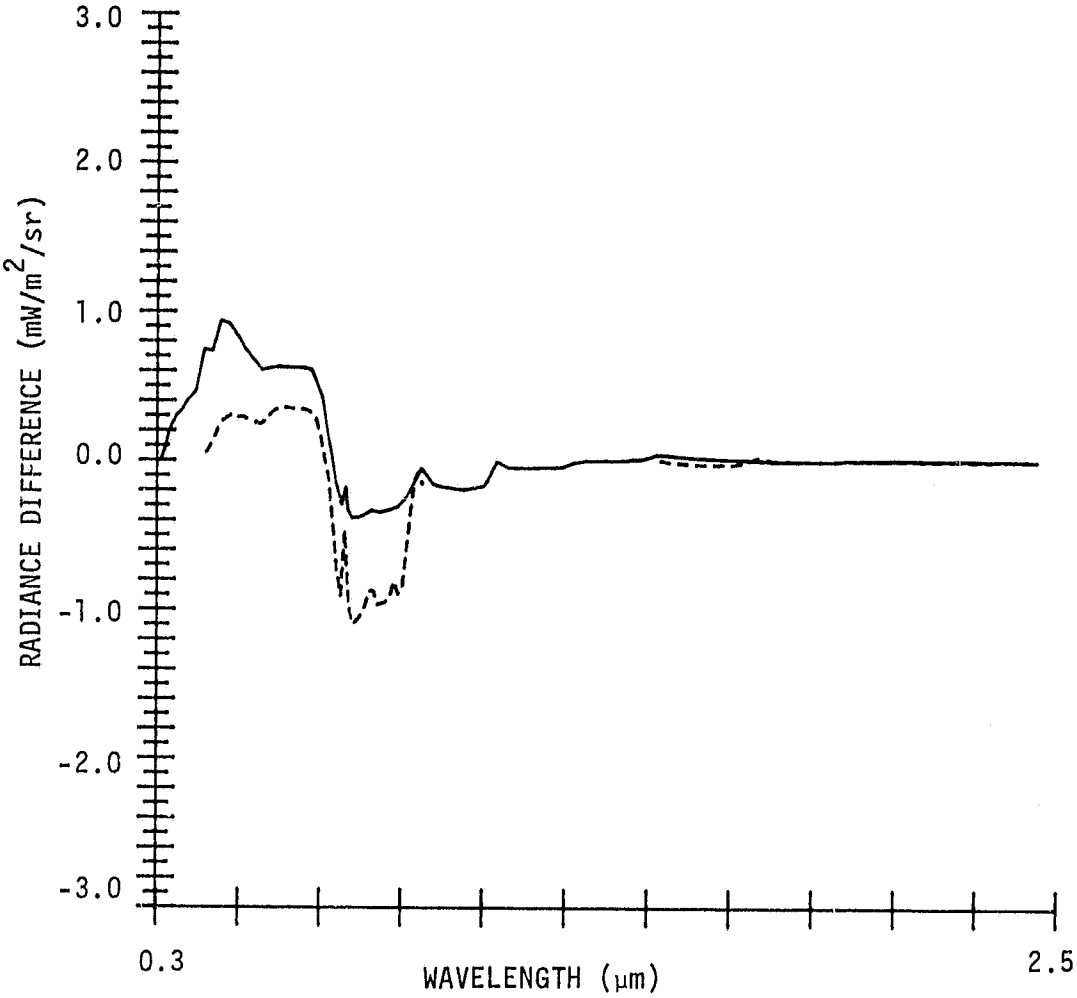

FIGURE 3.6. DIFFERENCE BETWEEN HAZY AND CLEAR CONDITIONS - OTHER PARAMETERS VARYING, WHEAT SPECTRUM #2

KEY: —— = Dave, — — = Turner

b) Averaged Background, 45^{o} Sun

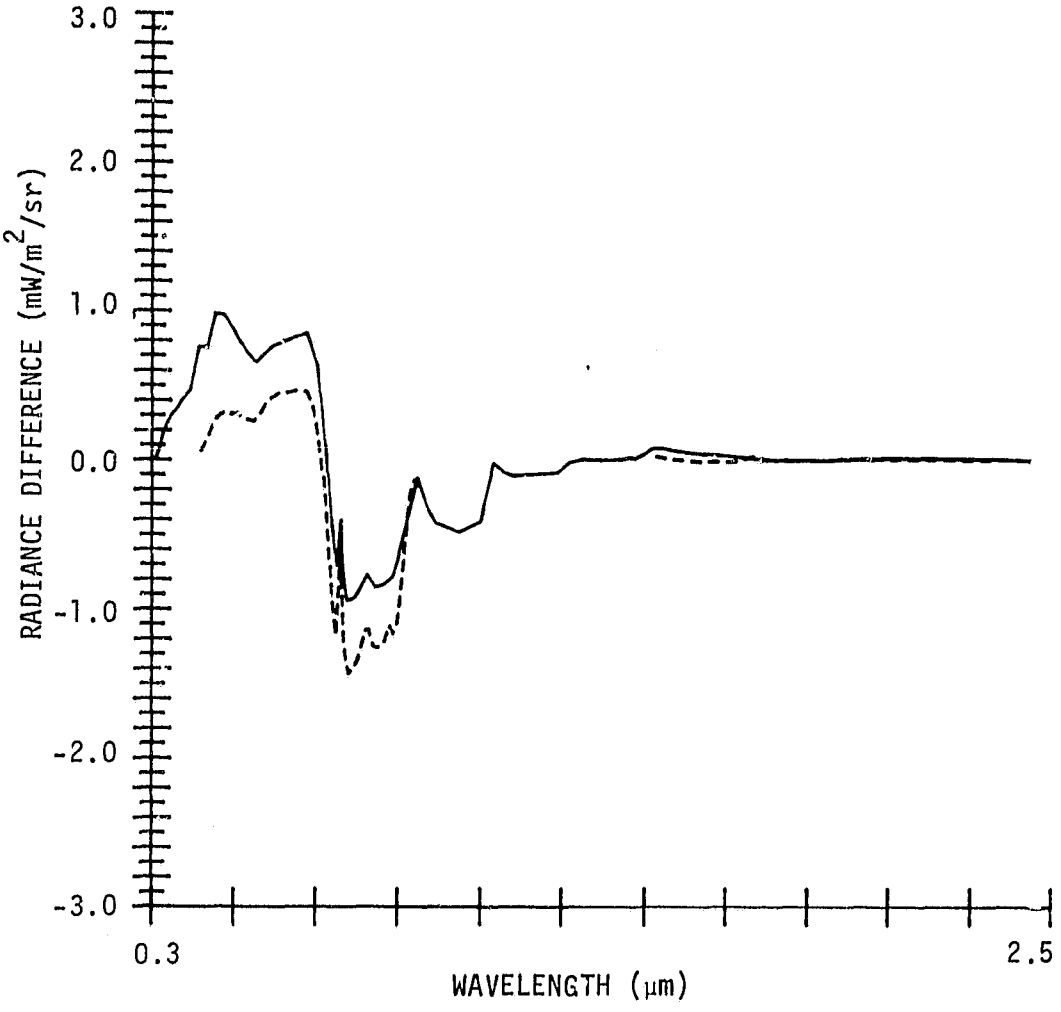

FIGURE 3.6. DIFFERENCE BETWEEN HAZY AND CLEAR CONDITIONS - OTHER PARAMETERS VARYING, WHEAT SPECTRUM #2 (Continued)

c) Averaged Background, 30° Sun

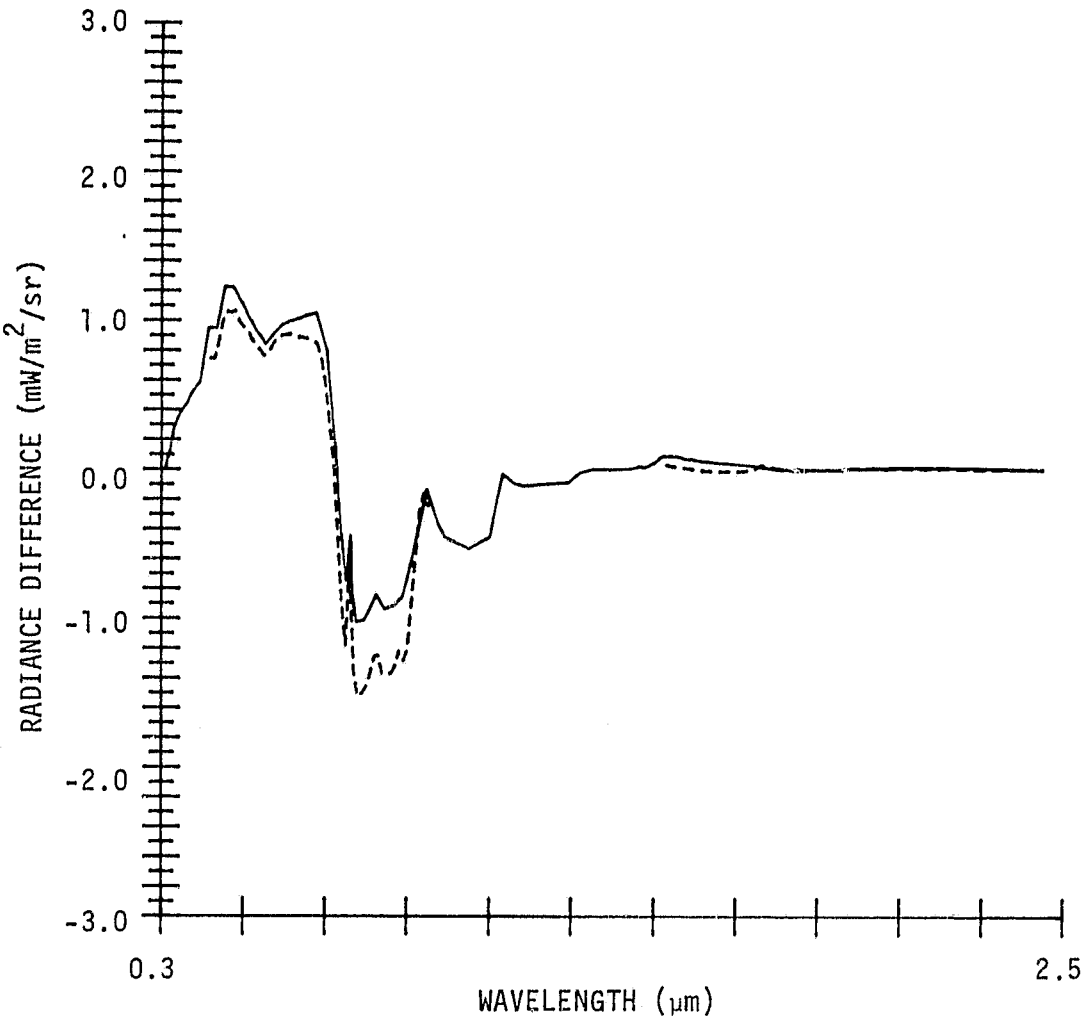

FIGURE 3.6. DIFFERENCE BETWEEN HAZY AND CLEAR CONDITIONS - OTHER PARAMETERS VARYING, WHEAT SPECTRUM #2 (Continued)

of conditions. The topmost graph (Figure 3.6a) shows the shifts predicted by the Dave and Turner models assuming that background reflectance equals target reflectance and with a solar zenith angle of 45 degrees. In the second graph (Figure 3.6b) the averaged soil and wheat spectrum is used in computing background reflectance. The effect is an improvement in the correlation between the two models in the 0.7 to 0.9 μm range. This improvement results from the fact that the composite background is less reflective than the target. Thus the relative underestimation, in the Turner model, of the contribution of background reflectance affects a smaller fraction of the total signal, and so the results from the two models are more similar. Finally, the last graph (Figure 3.6c) presents the results using composite background reflectance and a 30 degree solar zenith angle. The result of higher illumination source is significantly improved correlation of the 0.4 to 0.7 μm range. This result is consistent with previous studies which have suggested that the Turner model is most accurate for sun zenith angles in this range [11].

3.1.4 STATUS AND PLANS

Results to date clearly indicate that the QSS and Iterated Eddington Approximation models in the form available to this task are inadequate for the planned analyses. Accordingly, little or no further consideration will be given to these models. The Turner model seems to compare favorably to the Dave model for the most part, although it does deviate from that model in particular circumstances and wavelengths. Further comparisons will emphasize: 1) determining those conditions (especially illumination geometry) which minimize the model differences and 2) determining whether any particular scene classes are associated with greater disparity in model results. The Turner model will then be applied to the task of corroborating and/or refining the results of the haze effects analysis and haze diagnostic derivation carried out using the Dave data sets (Sections 3.2 and 3.3).

3.2 DAVE MODEL ANALYSES

3.2.1 DATA SET AND APPROACH

Dave Models 1 through 4, described in Table 3.1, were used with the crops and soils spectral data base described in [12]. Models 3 and 4, the two complete atmospheres representing very clear and moderately haze conditions respectively, were run at sun elevation angles of 30^{o}, 45^{o} and 60^{o}.

The output from the various model configurations was converted to TM Tasseled Cap features, plotted and analyzed through linear regression. Residual analysis was carried out on a selection of cases to determine whether the linear regressions could be treated as valid.

3.2.2 HAZE EFFECTS

Figure 3.7 shows the effects of haze on data distributions in the TM Tasseled Cap "Fundamental Views". Increasing haze tends to increase the Brightness of all but the highest Brightness data points, while decreasing Greenness values and increasing Wetness values. The Plane of Vegetation effects are consistent with those observed in MSS data [13]. The associated regression equations, presented in Table 3.2, illustrate the relative magnitude of effect for the three TM Tasseled Cap features. Brightness shows the strongest overall influence, particularly in the additive term, while Wetness is least affected. Average changes in signal values from clear to hazy atmosphere for the three features were 10, -9 and 5 counts for Brightness, Greenness and Wetness. Residual plots showed no gross deviations from linearity.

TABLE 3.1. DESCRIPTION OF DAVE MODEL DATA SETS

Model	Characteristics
1	Rayleigh scattering only
2	Model 1 + gaseous absorption
3	Model 2 + aerosol scattering and absorption
4	Model 3 with 5x greater aerosol density

TABLE 3.2. REGRESSION COEFFICIENTS FOR HAZE EFFECTS ANALYSIS

Model 4 (hazy) regressed on Model 3 (clear)
(45^{0} sun zenith angle)

Feature	Multiplicative Term	Additive Term
Brightness	0.89	19.5
Greenness	0.87	-5.1
Wetness	0.96	3.4

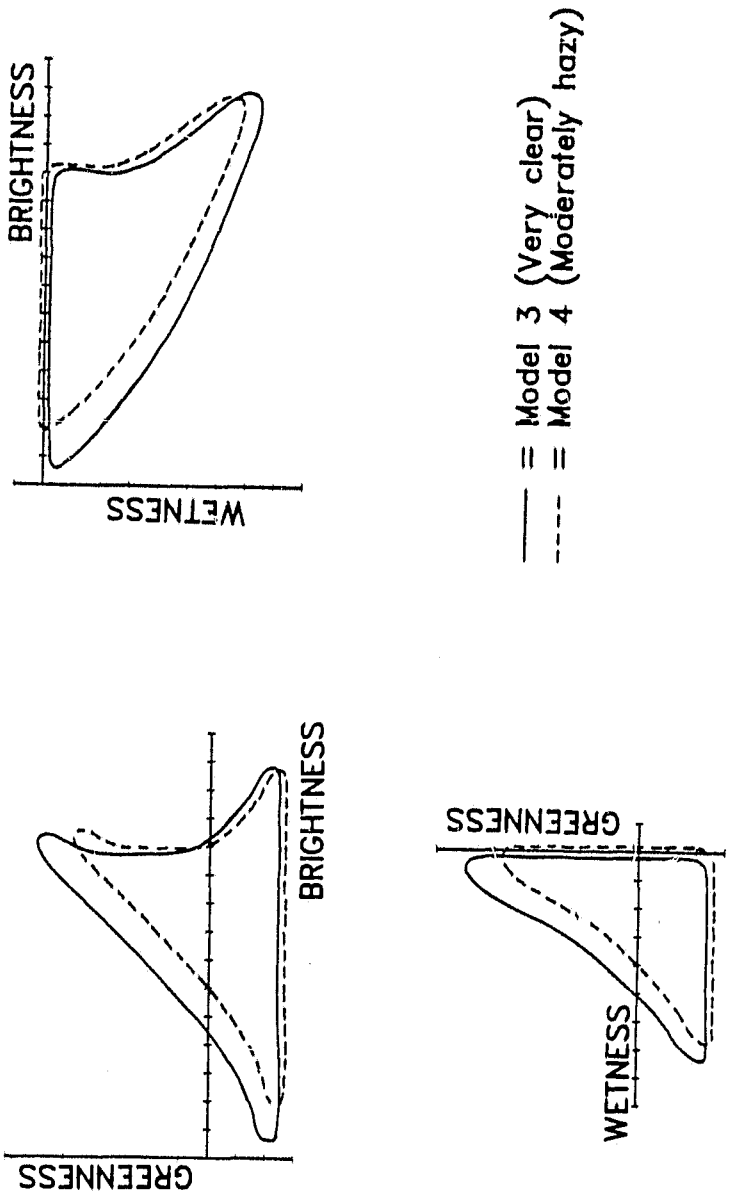

FIGURE 3.7. THEMATIC MAPPER HAZE EFFECTS

3.2.3 SUN ZENITH ANGLE EFFECTS

Figure 3.8 illustrates sun zenith angle effects using a clear atmosphere (Model 3). The associated regression coefficients are provided in Table 3.3. As is evident from the table, the coefficients are similar, though not identical, to the correction factors computed using the cosine of the sun zenith angles, i.e.,

$$x' = \frac{\cos\theta(1)}{\cos\theta(2)} * x$$

where

x = initial data value, sun zenith angle $\theta(2)$
x' = estimated data value, sun zenith angle $\theta(1)$

Again, residual plots gave no indication of gross nonlinearities.

3.3 HAZE FEATURE DERIVATION

In order to correct or normalize the effects of atmosphere on sensor data, a means must be found by which the haze condition of a particular scene or portion of a scene can be ascertained. In MSS data, the Tasseled Cap feature Yellowness, which primarily contrasted the two shortest wavelength bands (green and red), was used as a diagnostic feature [13]. This work was aimed at determining the potential for a similar feature in TM Tasseled Cap space.

A good haze diagnostic should have two characteristics: it should be insensitive to changes in scene content, and it should exhibit maximum sensitivity to changes in atmospheric conditions. Since about 99% of the variation in the simulated data set was contained in the first three TM Tasseled Cap features, the fourth through sixth features were used in deriving the haze diagnostic. However, some soils

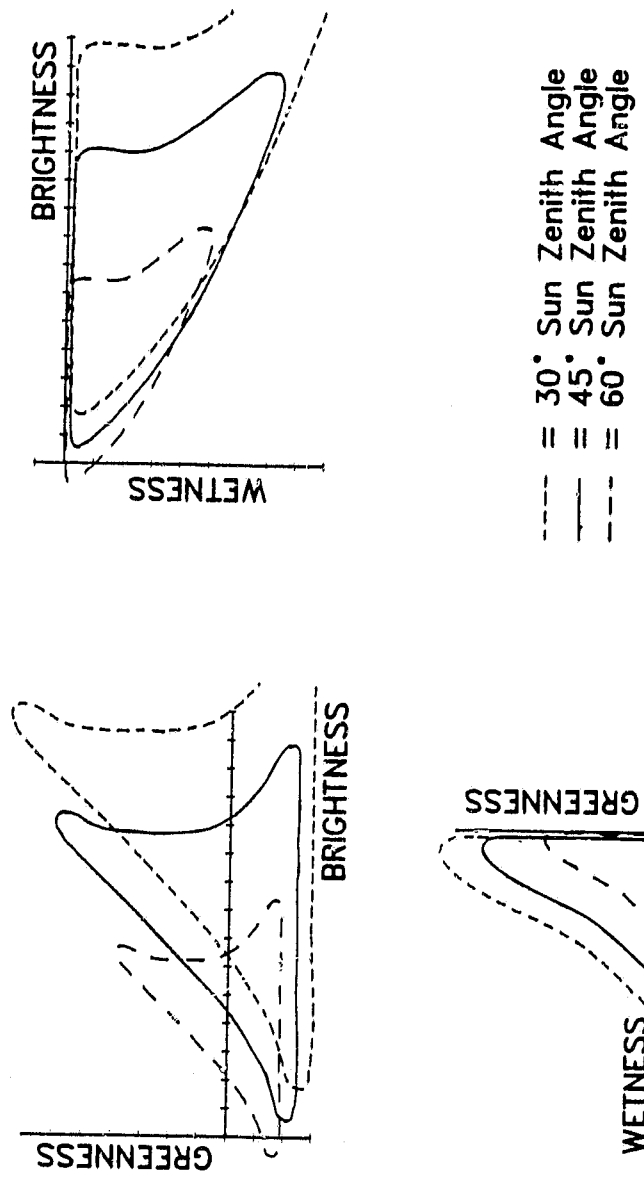

FIGURE 3.8. THEMATIC MAPPER SUN ZENITH ANGLE EFFECTS

TABLE 3.3. REGRESSION COEFFICIENTS FOR SUN ZENITH ANGLE EFFECTS ANALYSIS

Model 3 - Clear Atmosphere

30^{o} regressed on 45^{o} (cosine correction = 1.225)

Feature	Multiplicative Term	Additive Term
Brightness	1.25	-2.5
Greenness	1.24	0.8
Wetness	1.24	0.1

60^{o} regressed on 45^{o} (cosine correction = 0.707)

Feature	Multiplicative Term	Additive Term
Brightness	0.68	5.3
Greenness	0.68	-2.0
Wetness	0.69	0.8

variability was apparent in the fourth feature as well. Because this feature contains a significant contribution from the shortest wavelength TM band, which should be sensitive to atmospheric conditions, it was not deemed wise to delete it from consideration. Instead, only vegetated data were used in the analysis. This stratification solved the problem of soil variation in the feature space, and should be easily accomplished with actual data based on Greenness values.

Using the vegetated data in the fourth through sixth features, differences were computed between data viewed through the clear and hazy atmospheres. Principal components analysis was then applied to these differences, resulting in the primary directions of spectral change in response to changes in atmospheric haze. The diagnostic feature thus derived, which accounted for 67% of the total haze-related variation, has the following coefficients:

TM Band	1	1	3	4	5	7
	-.8836	.0565	.4438	.0151	.0029	.1373

Figure 3.9 shows the distribution of this haze diagnostic feature for the four Dave models at a common sun zenith angle. Most important is the difference between the Model 3 (clear) and Model 4 (hazy) results - the distribution means are more than four standard deviations apart, with no overlap between the $\pm$ 2 standard deviation intervals. The average data shift between the two models is 10 counts, or greater than three standard deviations of either distribution.

Even between Model 2, which has no aerosol component, and Model 3, which has a small aerosol component, an average shift of one standard deviation occurs. Thus it appears that this feature offers promise of providing useful haze-related information which could be used in correcting TM data.

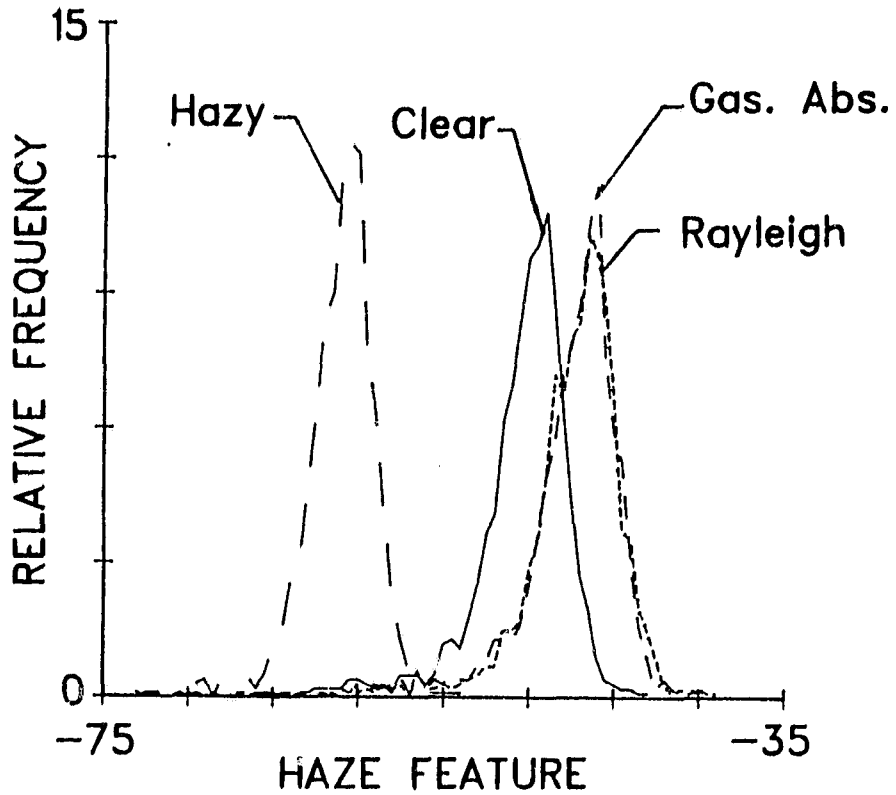

FIGURE 3.9. SIMULATION-BASED HAZE DIAGNOSTIC FEATURE

4.0
THEMATIC MAPPER TARGET SIGNATURE CHARACTERIZATION

Understanding the basic dimensional relationships in sensor data (Section 2.0) and the effects of external conditions such as atmospheric haze on those data (Section 3.0), one must still be able to extract meaningful information from the data in order for those data to be of any real use. This section describes research aimed at understanding the patterns of spectral development characteristic of particular scene classes, as well as deriving means by which other relevant scene class information may be extracted from TM data.

4.1 CROP PROFILE CHARACTERIZATION

The changes in geometry and composition which occur as a vegetative canopy develops are logically accompanied by changes in the spectral response of that canopy. Particularly in agricultural inventory applications, the patterns of spectral development, termed profiles, have been found to be of significant utility in distinguishing between various cover types. Since the primary TM data domain is three-dimensional rather than two-dimensional, as was the case with MSS data (see Section 2.0), the potential exists that even more developmental information will be available from TM data.

Figure 4.1 illustrates a general pattern of development for annual vegetation. The starting point is bare soil - on the "soil line" in the Plane of Vegetation view (point a in Figure 4.1a), and somewhere in the Plane of Soils, depending on the reflectance characteristics and moisture status of the soil (point a in Figures 4.1b and 4.1c). As plants begin to emerge from the soil, their spectral characteristics begin to cause an increase in Greenness while the shadow they cast will, unless the soil itself is very dark, tend to cause a decrease in Brightness. Addition of vegetative matter also tends to drive the field toward the Plane of Vegetation (in the Transition Zone view of

FIGURE 4.1. GENERALIZED CROP DEVELOPMENT PATTERN IN TM TASSELED CAP SPACE

Figure 4.1c). Continued green vegetation development causes these trends to continue, to the point at which the soil is completely obscurred from view. At this point the field is on the "green arm" (point c in Figure 4.1a) and in the Plane of Vegetation (point c in Figures 4.1b and 4.1c). Additional green vegetation beyond this point reduces visible shadows and increase the depth of stacking of green leaves, resulting in an increase in both Greenness and Brightness. This is expressed as movement up the green arm and within the Plane of Vegetation.

The onset of senescence results in a decrease in Greenness, while the effect on Brightness varies with vegetation type. In Figure 4.1, the senescent canopy consists of densely packed, highly reflective plant parts (typical of grasses and small grains), so the Brightness component increases as those plant parts occupy an increasingly larger portion of the canopy. Senescence as seen in the Transition Zone and Plane of Soils views (Figures 4.1b and 4.1c) tends to occur within the Plane of Vegetation, indicating offsetting changes in reflectance in the two wavelength regions contrasted in Wetness (see Section 2.0). Thus until the very end of the senescence phase, the field tends to remain in the Plane of Vegetation, venturing out toward the Plane of Soils only as full maturity is reached.

From the preceeding discussion, one key improvement can be seen resulting from the third dimension of information available in TM data. In the Plane of Vegetation view (Figure 4.1a), which corresponds to the MSS data plane, it is virtually impossible to distinguish, with a single acquisition, between a field that is "greening-up" and is thus a mixture of green vegetation and soil, and a field that is beginning to senesce, and thus shows a mixture of green and brown vegetation. Both of these processes occupy the same spectral region in Brightness-Greenness space. In the Transition Zone view, however, the two can be separated. A field that is "greening-up" will not yet have reached the Plane of Vegetation, falling instead somewhere in the Transition Zone between the two planes. A senescing field, however,

will fall in the Plane of Vegetation, and will remain there until the very end of the senescence process. The ability to distinguish these two transitional stages should significantly enhance our ability to determine the approximate stage of vegetative development from a single acquisition, and thus provide improved information for determining vegetation type or condition.

While useful information can be obtained, as described above, from the general patterns of vegetative development depicted in Figure 4.1, distinguishing between vegetation types involves more subtle variations in the development patterns, related to differences in canopy geometry, growth habit and development cycle. Using a cubic smoothing spline algorithm [14], a first level effort has been carried out to characterize profiles for two important agricultural crops: corn and wheat. Figure 4.2 provides an example result from this analysis. The Greenness and Brightness profiles are consistent with those observed in MSS data, as would be expected. The Wetness profile, which supplies information not available from MSS data, is consistent with the general pattern of development described previously. While the data used in this study do not support any definitive conclusions with regard to crop profile separability, the results do suggest that, as with MSS data, a profile-based approach to classification of vegetative types could be of value. Further study, with a larger data set, should be carried out to characterize the profiles of important cover types and to test the concept of profile-based classification using TM Tasseled Cap data.

4.2 TRACKING PERCENT VEGETATIVE COVER

As is clear from the discussions in Sections 2.0 and 4.1, the relative mix of vegetation and soil in the sensor field of view is expressed by the relative location of the data point in the Transition Zone between the Planes of Soils and Vegetation. Plotting distributions of percent vegetative cover in this data projection, as

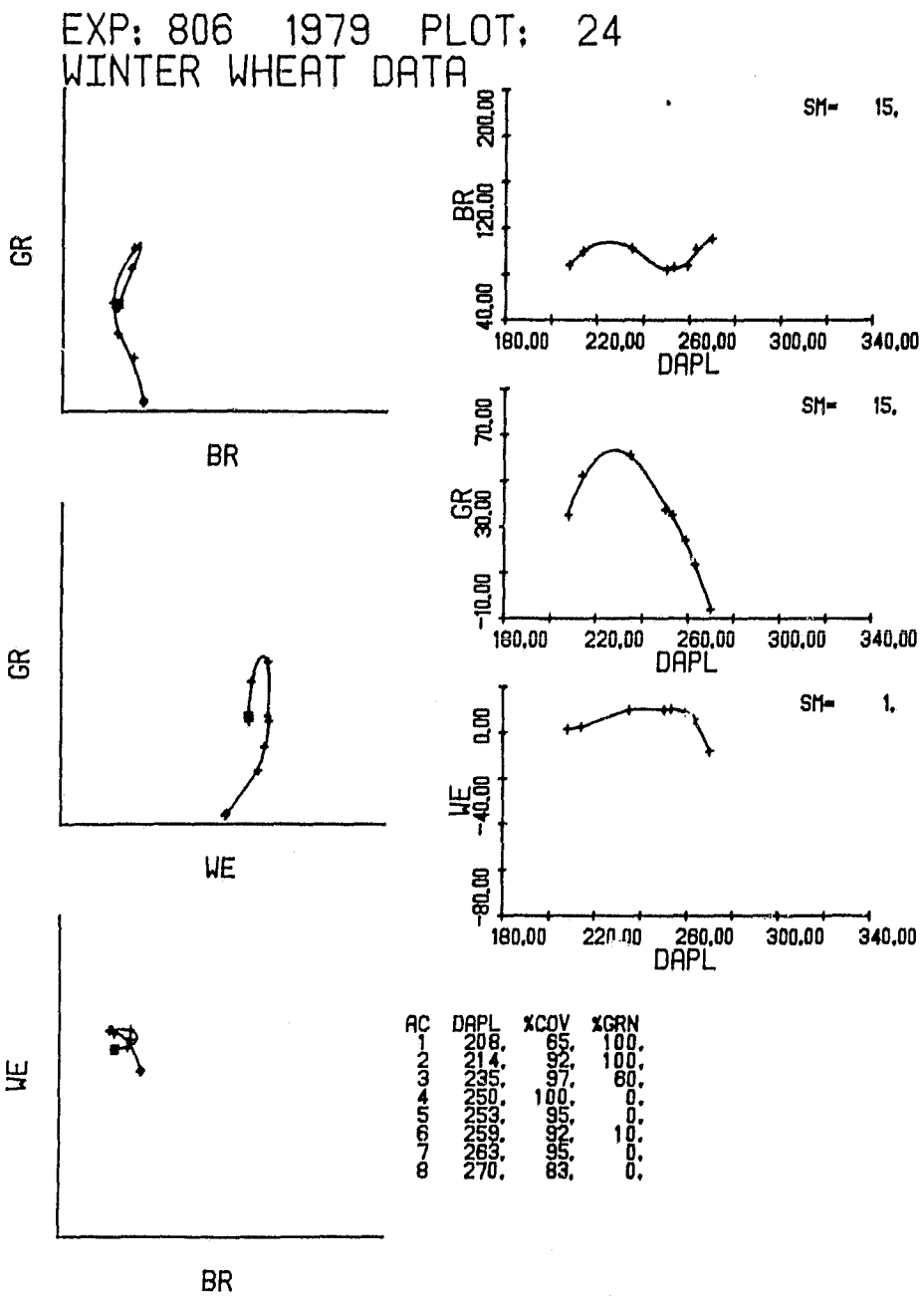

FIGURE 4.2. EXAMPLE WINTER WHEAT PROFILES

in Figure 4.3, one can see the trend from bare soil to full vegetative cover.

A simple method to more directly relate signal in this projection to percent cover is illustrated in Figure 4.4. Here an angle, termed the Transition Angle, is computed from the negative Wetness axis, such that an angle of 0^{o} indicates a data point on the Plane of Soils and an angle of 90^{o} indicates a data point on the Plane of Vegetation. Computing this measure for all the data in the simulated data set [1] yields results as depicted in Figure 4.5. Although the pattern is different for the three crops (a fact which may itself be exploitable in crop discrimination), in all cases this simple measure seems to yield good results.

Other measures, such as ratios or angles between TM bands 4 and 3 or between Greenness and Brightness, yield somewhat similar results. While no overwhelming superiority can be claimed for the new technique, two obvious advantages do present themselves. First, the other ratios tend to saturate, i.e., become insensitive to changes in percent cover at a certain point, or continue to increase after full cover has been achieved. Because the Transition Angle is constrained between two relatively static data structures (the Planes of Vegetation and Soils) which are associated with 0% and 100% vegetative cover respectively, it does not saturate, nor does it change after full cover has been achieved.

Second, the planar structure of the TM data is such that the Transition Angle falls in a convenient 0 to 90^{o} range, allowing easy interpretation of results. The band ratios and angles, on the other hand, fall in a less well-defined range, with maximum cover being associated with a green arm whose precise angular location is difficult to determine.

It appears, then, that the Transition Angle provides improved ability to extract information with regard to the relative mix of soil and vegetation causing a particular signal value. Such information can be of considerable use in interpreting vegetation development and

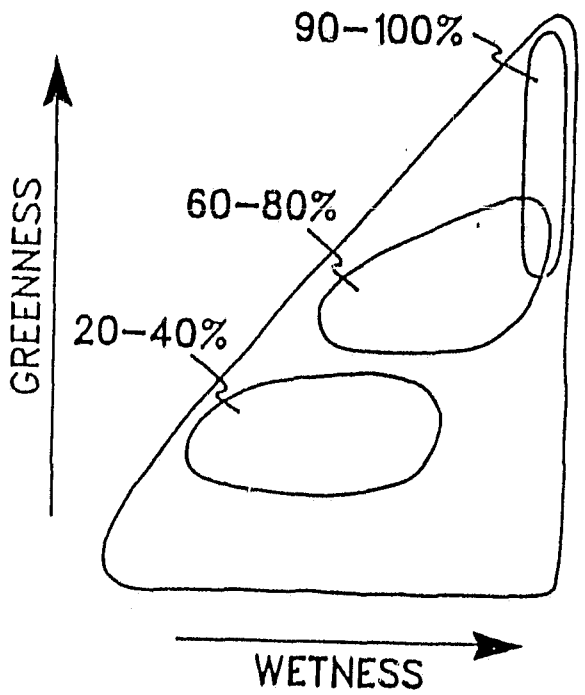

FIGURE 4.3. PROGRESSION OF SIMULATED DATA (COMPLETELY GREEN VEGETATION) THROUGH TRANSITION ZONE AS A FUNCTION OF PERCENT VEGETATION IN THE FIELD OF VIEW

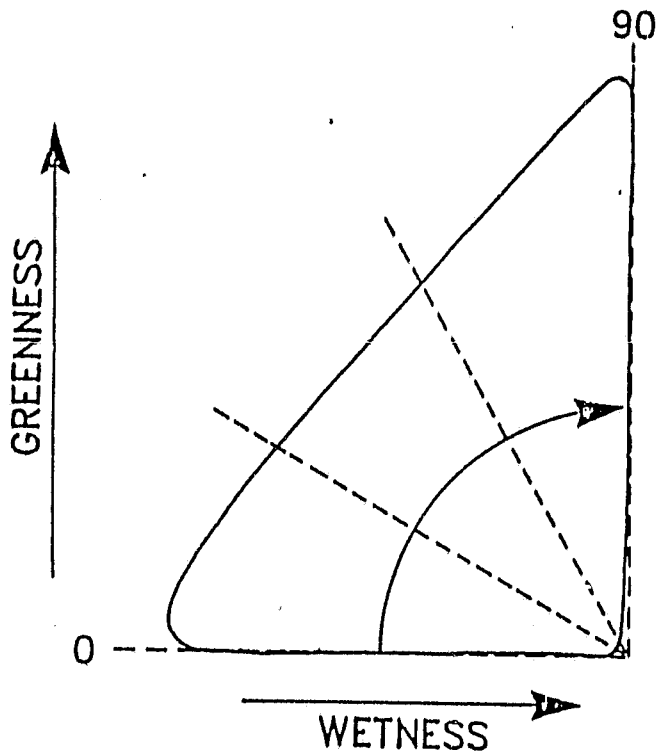

FIGURE 4.4. DEFINITION OF TRANSITION ANGLE

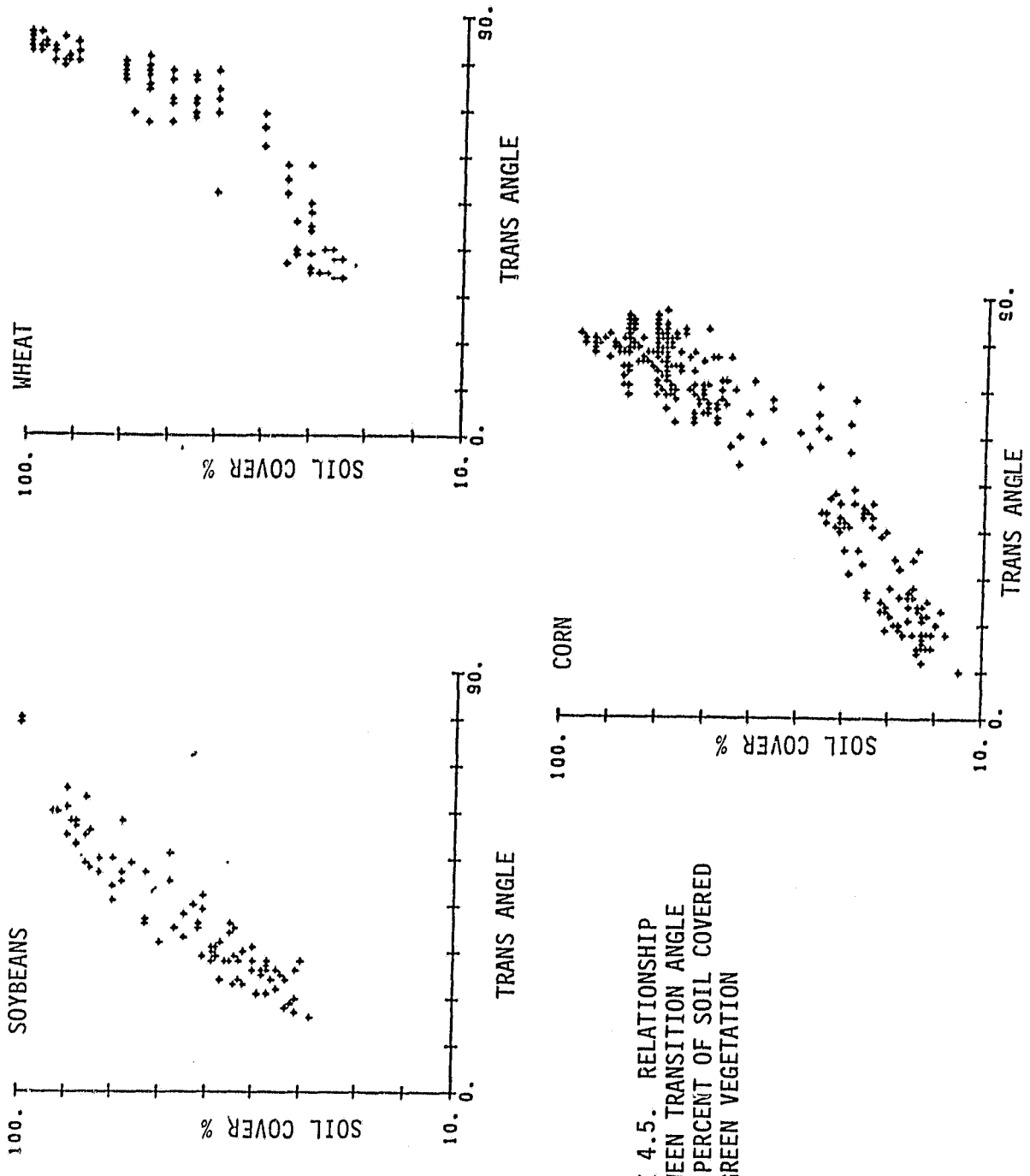

FIGURE 4.5. RELATIONSHIP BETWEEN TRANSITION ANGLE AND PERCENT OF SOIL COVERED BY GREEN VEGETATION

condition, as well as in separating the spectral influence of soil and vegetation. Further analysis of vegetative effects in the Transition Zone, and investigation of the spectral effects of changes in soil conditions under partial vegetative cover, should be carried out in order to more fully understand and utilize such information in an operational setting.

5.0
THEMATIC MAPPER THERMAL BAND INVESTIGATIONS

The launch of Landsat-4 with its seven-band Thematic Mapper presented investigators with new tools for observing the earth. In particular, the 10.4 to 12.5 μm thermal band provides high-resolution (120-meter) imagery coincident with visible and near- infrared data. Although previous systems have had spectral bands in the thermal range, they have not been widely used in conjunction with visible and near-infrared data. In the case of the Landsat-3 MSS, the thermal band did not function properly, while for the NOAA/AVHRR sensors, the thermal bands are 1100-meter resolution and have been used primarily for cloud detection.

The overall objective of this task was to increase our understanding of the characteristics and potential of the Thematic Mapper thermal band. To this end, two subtasks were initiated. The first was a simulation study aimed at describing atmospheric and scan-angle effects on TM thermal band radiometry. The second subtask developed local and global energy balance models based on Thematic Mapper data, then applied those models to a sample TM scene to demonstrate the feasibility of the technique. Details of these investigation are provided in the following sections.

5.1 ANALYSIS OF EXTERNAL EFFECTS ON TM THERMAL DATA

Understanding of the characteristics of the TM thermal band is essential to development of techniques which utilize this band in land use analysis. The LOWTRAN 5 model [15] provides an accurate simulation capability in the thermal region, and was therefore used as a source of controlled data by which TM thermal band properties could be explored.

Using calibration information obtained from NAsA/GSFC, TM signal counts were converted to apparent temperature. An investigation was then begun to determine the effects of varying atmospheres and scan

angle parameters on the apparent temperatures. The configuration of the LOWTRAN 5 model as used in these analyses is defined in Table 5.1.

Using the described model configuration with a nadir view, simulated targets appeared 4.2^{o} cooler than they would have without an atmosphere. When the visual range was varied, the effect was as described in Table 5.2. As would be expected, a smaller visual range (hazier atmosphere) had a greater effect on apparent temperature.

Holding atmospheric parameters constant while varying target temperature illustrates the range of error as a function of target condition. For the minimum detectable temperature of 260^{o}K, an apparent temperature measurement error of -0.6^{o}C was observed. This error increased essentially linearly to a -6.1^{o}C level for a 320^{o}K target (the maximum detectable temperature).

A third study held all parameters constant while varying the view angle. This study revealed that with the scan angle range of the TM, no significant effect on temperature measurement error occurs. That error increased only 0.06^{o}C from a nadir view (-4.25^{o}C error) to a view angle of 10^{o} (-4.31^{o}C error).

Finally, with a constant visual range, atmosphere and haze type were varied (e.g., continental vs. maritime). Within this group of conditions, errors ranged from -3.0^{o}C to -6.2^{o}C, suggesting the magnitude of error which might be incurred even if visual range were somehow taken into account.

As a result of these simple studies, one can conclude, albeit tentatively, that scan angle effects may be ignored in TM thermal data, but that atmosphere and haze type, and visual range, must be accounted for if accurate measurements of the apparent temperatures of targets are to be made.

Plans to test some of these results with actual TM data were developed, but were not carried out due to the previously mentioned redirection of effort.

TABLE 5.1. LOWTRAN 5 MODEL BASELINE CONFIGURATION

Atmosphere:	mid-latitude winter
Haze Type:	rural
Earth Temp:	300°K
Visual Range:	15 km
Sensor Location:	above atmosphere

TABLE 5.2. EFFECT OF VISUAL RANGE ON APPARENT TEMPERATURE

Visual Range	Effect on Apparent Temp. (°C)
1	-18.1
2	-11.2
3	-8.7
5	-6.6
10	-4.9
15	-4.2
25	-3.7
50	-3.3
100	-3.0
300	-2.9

5.2 USE OF THEMATIC MAPPER DATA FOR ENERGY BALANCE ANALYSIS

5.2.1 INTRODUCTION

The Thematic Mapper provides a temporal and spatial measure of thermal radiation which can be related to the temperature of the earth's surface. This information can in turn be utilized to both monitor the global energy balance and better understand local climatological trends. Both of these require knowledge of the radiation exchange between the earth and its surroundings. Understanding local climatological trends also requires the analysis of the exchange of energy between the atmosphere and land systems. The use of Thematic Mapper data for these analyses is discussed in more detail in Sections 5.2.2 and 5.2.3.

The earth's area included in a single frame of imagery is in a continually unsteady state. It gains energy during the day and loses it during the night. This diurnal variation is superimposed on a seasonal variation in most areas of the earth. Also, the land area is interacting with the atmosphere and other areas of the earth through atmospheric energy exchange. Thus the local energy balance problem is complex and will require analysis over a significant period of time in order to identify long term trends.

The global energy balance is somewhat simpler in the sense that the earth's atmosphere can be included as part of the earth and only net radiation exchange between the earth and the rest of the universe need be considered. However, because the energy content of different areas of the earth is continually changing, an analysis of the entire earth should be performed at a single instant in time in order to assess the global trends. Thus an effective and efficient sampling strategy will be of key importance in global energy balance monitoring.

5.2.2 GLOBAL ENERGY BALANCE

The earth's overall balance at any time is described by the following equation:

$$\Delta E = \{Q(\text{solar}) - Q(\text{solar reflected})\} - Q(\text{earth radiated}) + Q(\text{internally generated}) + Q(\text{other sources})$$

This equation states that the net change in energy of the earth is equal to the net solar radiation input to the earth less the radiation emitted by the earth plus the internally generated heat sources and energy absorbed from other stars and the moon. These latter terms are small. The left side of this equation represents the change in the overall earth's temperature and the storage of energy in vegetation. Over a long period of time, the change in the earth's temperature should be zero if there are no long-term global temperature trends.

The concern over a potential global earth temperature change in based on the Q(solar reflected) term ("Is the buildup of particulates in the atmosphere increasing this term?") and the Q(earth radiated) term ("Is the absorption of radiation by the increased carbon dioxide in the earth's atmosphere reducing the overall magnitude of this term?"). In order to address these questions one needs to evaluate the portion of the ΔE term related to the change in the Earth's overall temperature. This in turn requires sampling to identify the earth's overall energy balance at any moment. Such sampling must be repeated over a period of time in order to estimate the partitioning of energy storage into that stored naturally in vegetation and that stored as thermal energy in a changing global temperature. This problem is extremely difficult and beyond the scope of this program. However, a demonstration of the use of Thematic Mapper data for energy balance analysis, which is a part of the problem, is described in the next section.

5.2.3 LOCAL ENERGY BALANCE

In addition to the world's overall heat balance, the local earth's surface area temperature and energy balances are also of interest. The equation for a particular portion of the earth's surface is:

$$\Delta E = Q(\text{solar}) - Q(\text{solar reflected}) + Q(\text{conduction}) + Q(\text{radiation atmosphere}) - Q(\text{radiation ground}) - Q(\text{convection}) - Q(\text{evaporation})$$

For purposes of this discussion, Q(conduction), which is insignificant relative to the other terms, is ignored. Local areas of the earth's surface are continually changing temperature, so the ΔE term in the above equation is generally not zero. The earth's surface warms in the day, resulting in a positive ΔE term and cools at night, causing a negative ΔE term. Superimposed on this daily variation is the variation associated with seasonal changes in the upper four to six feet of the earth, with heat being stored in the Spring-Summer and lost in the Fall-Winter. In addition, depending on location, the growth of vegetation results in storage of energy in biomass.

Local areas interact with each other through the atmospheric and ocean currents which carry energy from the tropics to the polar regions. Consequently, in general, local surface regions are in a continual state of energy flux with storage or loss due to seasonal or meteorological variations.

A demonstration of the application of Thematic Mapper data to energy balance questions was carried out using the Iowa Frame (Scene #40049-16262) collected on 3 September 1982. Using a coarse segmentation of the data distribution in TM Brightness and Greenness, the ground cover was classified into five categories, as shown in Table 5.3.

TABLE 5.3. CLASSIFICATION OF IOWA TM SAMPLE

Bare Soil	- 0.95%
Water	- 0.94%
Green Vegetation	-86.47%
Brown Vegetation	-10.63%
Roads and Manmade Areas (rooftops, etc.)	- 1.01%

TABLE 5.4. SCENE AVERAGE REFLECTANCES

Band (μm)	Radiance (W/m^2 m)	Solar Input (W/m^2 m)	Reflectance
.45-.52	120.6	988.2	.122
.53-.60	96.1	895.5	.107
.63-.69	61.9	864.6	.071
.76-.90	281.8	494.1	.570
1.55-1.75	28.6	185.3	.154
2.08-2.35	4.7	43.2	.108

Using pre-launch calibration data, scene mean values in the TM bands were converted to radiance, and compared to a standard solar energy curve (based on location, time of year and time of day) to get average reflectance values in each TM band. This result is presented in Table 5.4. The average scene solar reflectance (i.e., based on the fraction of solar energy in each band as well as the reflectance) for this frame was thus 0.198, or approximately 20%. With the standard solar energy curve mentioned previously, this average mean reflectance was used to compute the net solar energy gain, which was 595.7 W/m^2. Again it should be noted that this number corresponds to the particular moment at which the data were collected (9:50AM, 3 September 1982, N. Central Iowa).

The remaining terms in the local energy balance equation were calculated using the following equations and local weather information as obtained from the National Weather Service. Radiation from the atmosphere was determined using the Idso-Jackson equation for atmospheric emmissivity and the local air temperature:

$$Q = \{1. - 0.261e^{(-7.77\times10^{-4}(2273 - T_a)^2}\}\gamma T_a^4$$

where

T_a = air temperature and
γ = Stefan-Boltzman constant

The radiation from the ground was calculated from the scene ground apparent temperature, as measured by the Thematic Mapper (after nominally correcting for atmospheric transmission and path radiance). The convection to the atmosphere is the sum of the forced and free convection and was calculated from the following expressions:

$$Q = hA(T_{ground} - T_{air})$$

where

h is the sum of the forced and free convection coefficients which are determined from

$$h_{free} = \frac{k}{L}(0.27(GrPr)^{1/4})$$

$$h_{forced} = \frac{k}{L}(.0322\ Re^{0.8})$$

where

k = thermal conductivity
L = significant length
Gr = Groshof number
Pr = Prandtl number
Re = Reynolds number based on wind speed, and

A is surface area

The evaporation term, which includes transpiration, was determined differently for various ground classes. For water areas, the calculation was:

$$V = C(E' - e)$$

where

V = rate of evaporation
C = a tabular function of wind speed
E' = saturated vapor pressure of water at the surface temperature

e = relative humidity x saturated vapor pressure of water at the air temperature

The rate of energy transfer was then calculated from the rate of evaporation and the heat of vaporization of water.

The rate of transpiration for green vegetation as computed from the following expression:

$$Q = h[P_{GV} - P_{SA}]$$

where

$$h = \frac{C_p P}{a(\frac{1}{r_1} + r_2)}$$

where

C_p = air specific heat
P = air density
a = conversion factor = .55 mm H_g/DF and
r_1, r_2 = diffusion resistances
P_{GV} = water vapor pressure at the vegetation temperature and
P_{SA} = saturated vapor pressure at the air temperature

The particular terms of the energy balance equation, and the rate of energy change of the land at the time of data collection are given in Table 5.5.

The Table 5.5, combined with the scene classification in Table 5.3, was used to calculate an overall rate of energy change for the test site. For this Iowa scene at the time of data collection, the net

TABLE 5.5. ENERGY BALANCE TERMS FOR TEST SITE

(all values in W/m^2)

	E	Q solar net	Q rad. in-out	Q conv.	Q evap.*
Bare Soil	480.3**	595.7	-82.3	-33.1	0.**
Water	305.4	595.7	-72.8	-33.1	-184.4
Green Veg.	286.5	595.7	-82.3	-145.6	-81.3
Brown Veg.	367.8	595.7	-82.3	-145.6	***
Man-made	480.3	595.7	-82.3	-33.1	

*Includes transpiration for green vegetation

**Depends on time since rain and water content of the soil

***May be significant given recent rainfall

scene energy content was increasing at the rate of 299.1 W/m^2. This rate is typical for rural areas at this latitude and time of day. Some of this energy is being stored as biomass, and some is raising the temperature of the ground and air. Much of the latter portion will be lost back to the universe during the night.

6.0
OTHER ACTIVITIES

Two research topics are discussed in this section. First, Section 6.1 describes the final elements of a task begun and largely reported in FY82, related to the effects on MSS data of various preprocessing techniques. Second, Section 6.2 describes work carried out to better understand the characteristics of another sensor, the NOAA Advanced Very High Resolution Radiometer (AVHRR) and to devise methods for its joint use with Landsat. This task was discontinued prior to completion so that effort could be directed toward other of the objectives of the Earth Sciences and Applications Division at NASA/JSC.

6.1 EFFECTS OF PREPROCESSING OF LANDSAT MSS DATA

Research carried out in FY82 under the auspices of the AgRISTARS program included an analysis of the relative merits and attributes of three approaches to normalization of sensor calibration, illumination geometry and atmospheric haze effects on MSS data [1]. As a follow-on to that activity, which emphasized the techniques' effects on overall data distributions and relationships, an analysis was conducted to determine the relative sensitivity of the techniques to changes in scene content. Clearly a preprocessing technique to be used in situations where little a priori information is known with regard to scene content must behave more or less independently with respect to that scene content. The analysis considered three techniques: XSTAR haze correction [16,17], Cate Color Normalization [18] and Multiple Acquisition Mean Level Adjustment [1,19]. Typical temporal profiles for corn, soybeans and trees were derived by extracting scene mean values for each crop from a multitemporal set of Landsat MSS data from AgRISTARS segment 127/78, the same data set used in the previous work. This segment included data from both Landsats 2 and 3, and included several clear acquisitions and at least one variably-hazy acquisition.

Using the mean-based profiles for the three cover classes, five hypothetical scenes were constructed, each containing different proportions of the three classes (see Table 6.1). These hypothetical scenes were then processed under each of the three methods (because of the loss of spatial information in the hypothetical scenes, global XSTAR was used in place of spatially-varying XSTAR). The resultant data were further transformed using either the Normalized Difference [20], the Tasseled Cap transformation [13], or the Cate Invariant Color Cube transformation [18].

Figure 6.1 summarizes the results of this experiment. The nine plots shown represent various combinations of feature transformations and preprocessing techniques. On each plot, profiles are drawn for corn, soybeans and trees. The shaded area represents the range of values resulting from the five hypothetical scenes in Table 6.1. Wider shaded regions thus indicate greater sensitivity, on the part of the preprocessing technique, to scene content, whereas narrower shaded regions indicate greater stability in this regard. As can be seen, XSTAR exhibits little apparent sensitivity to scene content in the spectral features displayed, although its use of Tasseled Cap Yellowness as a haze diagnostic will result in sensitivity to scene-related variation in Yellowness. While such variation is not of much concern in vegetated scenes, it may be of greater concern in other scenes. Color Normalization exhibits substantial sensitivity in all features, particularly in the middle of the growing season. Multiple Acquisition Mean Level Adjustment shows intermediate sensitivity, improving on the Color Normalization results but not reaching the level of stability of the XSTAR procedure.

6.2 ANALYSIS OF NOAA/AVHRR DATA

The Advanced Very High Resolution Radiometers (AVHRR) on board the NOAA-6 and NOAA-7 satellites offer the potential of supplementing the Landsat MSS data frequently used for environmental monitoring. A

TABLE 6.1. PROPORTIONS OF COVER CLASSES IN HYPOTHETICAL SCENES

Scene	%Corn	%Soy	%Trees
1	62	32	5
2	80	10	10
3	10	80	10
4	10	10	80
5	33.3	33.3	33.3

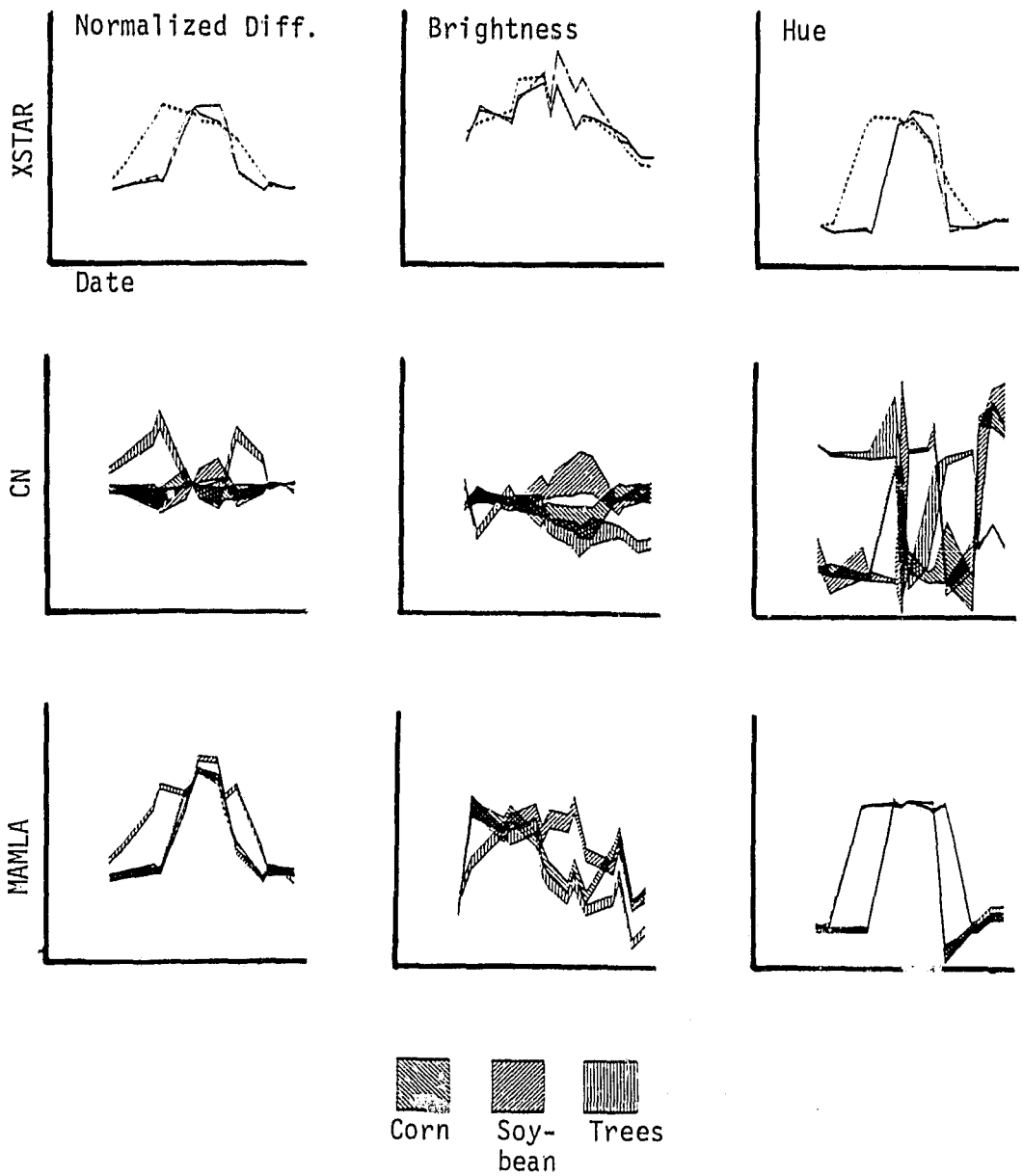

FIGURE 6.1. SENSITIVITY ENVELOPES OF NORMALIZED DIFFERENCE, BRIGHTNESS AND HUE

comparison of MSS and AVHRR system characteristics is presented in Table 6.2. While AVHRR has increased temporal coverage, its spatial and spectral resolution are much less that those of the MSS. For this reason, the joint use of the two sensor systems in a complementary fashion appears promising.

A limited effort was initiated which was directed at providing the base of understanding of AVHRR data necessary for such joint use. In particular, an understanding of the effects caused by the extreme scan angles was desired, as was the development of features similar to the Greenness and Brightness features previously developed for MSS data. Such feature development has been addressed at ERIM using simulated data [21], and elsewhere using actual AVHRR data [22-25]. This effort was intended to increase our understanding of the actual data, and therefore included some duplication of previous work.

To fully exploit the more frequent overpasses provided by the AVHRR, it is necessary to utilize a large portion of the scan. The full $\pm 56^{o}$ scan gives daily repeat, while restricting the portion of scan used to $\pm 10^{o}$ leads to repeat coverage every three days. For this reason, effort was directed at understanding the effects of the extreme scan angles on AVHRR data. A simple geometric model was developed which allows correction of pixel size as a function of sensor altitude and scan angle. Figure 6.2 illustrates the results of this model for the AVHRR. While this model addresses only the geometric effects of scan, additional, potentially severe radiometric effects due to bidirectional reflectance characteristics, optical path length changes and the sun-target-sensor angular relationship will still be present. Corrections for these effects were beyond the scope of this task.

Development of Greenness and Brightness-like features for the NOAA/AVHRR was intended to utilize a data set available on NASA/JSC's EODL system. Initial analyses indicated several limitations of this data set, including:

TABLE 6.2. SENSOR CHARACTERISTICS

	NOAA-7 AVHRR	Landsat 1-3 MSS
# Visible/Near IR Bands	2	4
Orbit Altitude	850 km	920 km
Equator Crossing	14:30	9:30
Nadir Ground Resolution	1100 m	79 m
Swath Width	2700 km	185 km
Field of View	$\pm 56^{o}$	$\pm 5.5^{o}$
Repeat Coverage	1 day	18 days

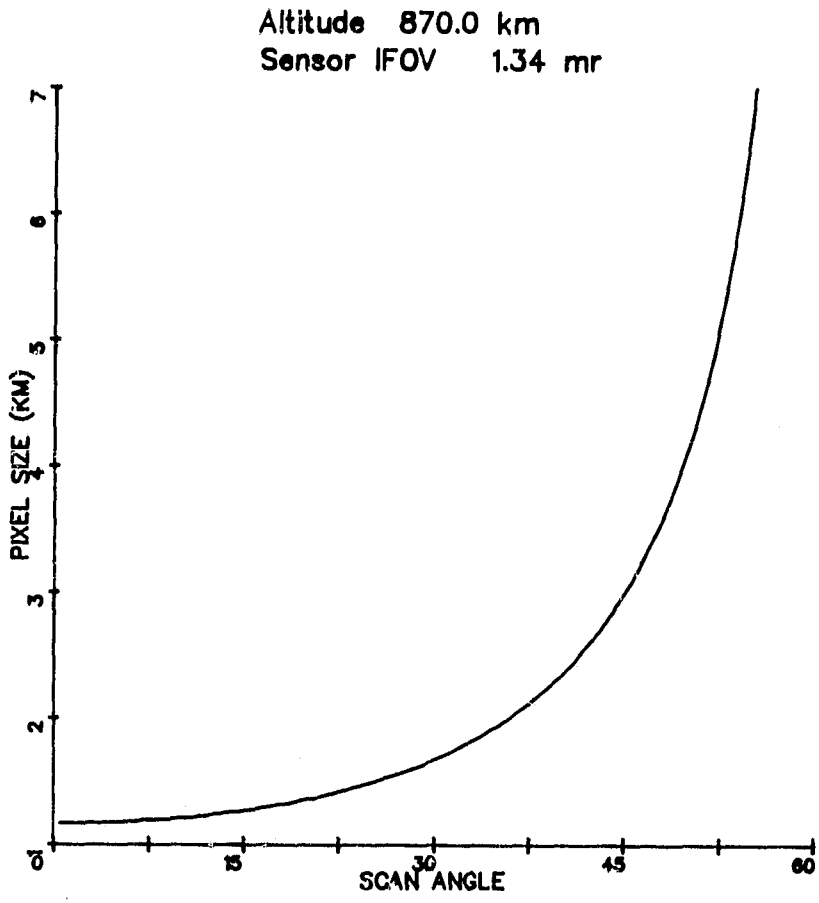

FIGURE 6.2. AVHRR PIXEL SIZE AS A FUNCTION OF SCAN ANGLE

(1) Data were already converted to "albedo" as per [26], and the calibration coefficients used were unavailable within the data set. As the majority of NOAA/AVHRR literature reviewed concerned analyses carried out on raw signal values, use of raw data was considered vital to this task.

(2) The processed (sun angle corrected and converted to albedo) data covered only the central 1404 pixels of 2048 pixel scan lines. This significantly reduced our ability to analyze the effect of extreme scan angles on derived features.

(3) Numerous anomolous values were present in the data (i.e., albedos greater than 200%). These anomolies reduced our confidence in the data set.

In consideration of these data limitations, and as a result of the need to redirect effort to other tasks, further work with this or other sets of actual AVHRR data was deferred.

REFERENCES

1. Cicone, R., E. Crist, M. Metzler and T. Parris. Development, Implementation and Evaluation of Satellite-Aided Aricultural Monitoring Systems, NASA Report IT-E2-04377, ERIM, Ann Arbor, MI, 1982.

2. Crist, E.P and R.C. Cicone. Application of the Tasseled Cap Concept to Simulated Thematic Mapper Data, Photogrammetric Engineering and Remote Sensing, 1984.

3. Crist, E.P. and R.C. Cicone. Comparisons of the Dimensionality and Features of Simulated Landsat-4 MSS and TM Data, Remote Sensing of Environment, pp.235-246, 1984.

4. Malila, W.A., M.D. Metzler and E.P. Crist. Study on Spectral/ Radiometric Characteristics of the Thematic Mapper for Land Use Applications, Fourth Type II Quarterly Status and Technical Report, NASA/GSFC, ERIM Report 164000-4-T, ERIM, Ann Arbor, MI, 1983.

5. Crist, E.P. The TM Tasseled Cap - A Preliminary Formulation, Proceedings of the Symposium on Machine Processing of Remotely Sensed Data, Purdue University, W. Lafayette, IN, 1983.

6. Crist, E.P. and R.C. Cicone. A Physically-Based Transformation of Thematic Mapper Data - the TM Tasseled Cap. IEEE Transactions on Geoscience and Remote Sensing, 1984.

7. Stoner, E.R. and M.F. Baumgardner. Physiochemical, Site, and Bidirectional Reflectance Factor Characteristics of Uniformly Moist Soils, Technical Report 11679, LARS, Purdue University, W. Lafayette, IN, 1980.

8. Dave, J.V. Extensive Datasets of the Diffuse Radiation in Realistic Atmospheric Models with Aerosols and Common Absorbing Gasses. Solar Energy 21:361-369, 1978.

9. Turner, R.E. Radiative Transfer in Real Atmospheres. NASA Report CR-ERIM 190100-24-T, 1974.

10. Herman, B., A.J. LaRocca and R.E. Turner. "Atmospheric Scattering", in Wolfe, W.L. and G.J. Zissis (editors), The Infrared Handbook, ERIM, 1978.

REFERENCES (Continued)

11. Lyzenga, D.R. Coastal Remote Sensing Investigations, Office of Naval Research, ERIM Report 134400-11-F, 1980.

12. Biehl, L.L., M.E. Bauer, B.F. Robinson, C.S.T. Daughtry, L.F. Silva and D.E. Pitts. A Crops and Soils Data Base for Scene Radiation Research. Proceedings of the Symposium on Machine Processing of Remotely Sensed Data, Purdue University, W. Lafayette, IN, 1982.

13. Kauth, R.J., P.F. Lambeck, W.R. Richardson, G.S. Thomas and A.P. Pentland. "Feature Extraction Applied to Agricultural Crops as Seen by Landsat", in Proceedings of the Technical Sessions, The LACIE Symposium, JSC 16015, NASA/Johnson Space Center, Houston, TX, Vol. II, pp.705-721, 1979.

14. Debour, C. A Practical Guide to Splines, Springer-Verlag, NY, 1978.

15. Kneizys, F.X., E.P. Shettle, W.O. Gallery, J.H. Chetwynd, Jr., L.W. Abreu, J.E.A. Selby, R.W. Fenn and R.A. McClatchey. Atmospheric Transmittance/Radiance: Computer Code LOWTRAN 5, Report No. AFGL-TR-80-0067, Air Force Geophysics Laboratory, USAF, Hanscom AFB, MI, 1980.

16. Lambeck, P.F. and J.F. Potter. Compensation for Atmospheric Effects in Landsat Data, Proceedings of the Technical Sessions, The LACIE Symposium, NASA/JSC, Houston, TX, October 1978, pp.723-738.

17. Lambeck, P.F. Spatially Varying XSTAR Haze Correction, NASA New Technology Report, ERIM, Ann Arbor, MI, March 1978.

18. Cate, R.B., D.E. Phinney, M.C. Kinsler, M.L. Sestak, T. Hodges and J.J. Dishler. Interpretation of Landsat Digital Data Using a Cubic Color Model Based on Relative Energies, NASA Report SR-LO-00418, LEMSCO, Houston, TX, February 1980.

19. Parris, T. and R.C. Cicone. Effects of Preprocessing Landsat MSS Data on Derived Features, Proceedings of the Symposium on Machine Processing of Remotely Sensed Data, June 1983, pp.170-178.

20. Rouse, J.W., R.H. Haas, J.A. Schell and D.W. Deering. Monitoring Vegetation System in the Great Plains with ERTS. Third ERTS Symposium, NASA SP-351, I:309-313, May 1975.

REFERENCES (Continued)

21. Cicone, R.C. and M.D. Metzler. Development of Common Features for Multi-Satellite Agricultural Information Extraction. Remote Sensing of Environment, pp.257-265, 1984.

22. Schneider, S.R., D.F. McGinnis, Jr. and J.A. Gatlin. Use of NOAA/AVHRR Visible and Near-Infrared Data for Land Remote Sensing. NOAA Technical Report NESS84, 1981.

23. Duggin, M.J. and D. Piwiaski. Study to Assess the Importance of Errors Introduced by Applying NOAA 6 and 7 AVHRR Data as an Estimator of Vegetative Vigor: Feasibility Study of Data Normalization. NASA Final Report on Contract 9-1663, 1982.

24. Duggin, M.J., D. Piwiaski, V. Whitehead and G. Ryland. Evaluation of NOAA-AVHRR Data for Crop Assessment. Applied Optics, 21:1873-1875, 1982.

25. Gray, T.I. and D.G. McCrary. Meteorological Satellite Data - A Tool to Describe the Health of the World's Agriculture. AgRISTARS Report EW-NI-04042, 1981.

26. Kidwell, K.B. NOAA Polar Orbiter Data Users Guide. Department of Commerce, National Climatic Center, Satellite Data Services Division, 1979.

APPENDIX A

ERIM PAPERS RELEVANT TO REPORTED TOPICS

Crist, E.P. The Thematic Mapper Tasseled Cap - A Preliminary Formulation, Proceedings of the Symposium on Machine Processing of Remotely Sensed Data, 21-23 June 1983.

Crist, E.P. and R.C. Cicone. Investigations of Thematic Mapper Data Dimensionality and Features Using Field Spectrometer Data, Proceedings of the 17th International Symposium on Remote Sensing of Environment, 9-13 May 1983 and delivered at AgRISTARS Mini-Symposium, 1-2 December 1982.

Crist, E.P. and R.C. Cicone. Application of the Tasseled Cap Concept to Simulated Thematic Mapper Data, Photogrammetric Engineering and Remote Sensing, 1984.

Crist, E.P. and R.C. Cicone. Comparisons of the Dimensionality and Features of Simulated Landsat-4 MSS and TM Data, Remote Sensing of Environment, pp.235-246, 1984.

Crist, E.P. and R.C. Cicone. Thematic Mapper Spectral Dimensionality and Data Structure. Proceedings of the Landsat-4 Early Results Symposium, 1984.

Crist, E.P. and R.C. Cicone. A Physically-based Transformation of Thematic Mapper Data - the TM Tasseled Cap. IEEE Transactions on Geoscience and Remote Sensing, 1984.

Parris, T. and R.C. Cicone. Effects of Preprocessing Landsat MSS Data on Derived Features, Proceedings of the Symposium on Machine Processing of Remotely Sensed Data, 21-23 June 1983.

APPENDIX B

OTHER ERIM PAPERS WRITTEN DURING REPORTING PERIOD

Metzler, M.D. and R.C. Cicone. Assessment of Technologies for Classification of Mixed Pixels, Proceedings of the 17th International Symposium on Remote Sensing, 9-13 May 1983.

Metzler, M.D., J. Odenweller, R.C. Cicone and K.I. Johnson. Experiments with an Expert-Based Crop Area Estimation Technique for Corn and Soybeans, Proceedings of the 17th International Symposium of Remote Sensing, 9-13 May 1983 and presented at AgRISTARS Mini-Symposium, 1-2 December 1982.